INTERNATIONAL CENTRE FOR THEORETICAL PHYSICS
LIBRARY

INTERNATIONAL ATOMIC ENERGY AGENCY
UNITED NATIONS EDUCATIONAL, SCIENTIFIC AND CULTURAL ORGANIZATION

INTERNATIONAL CENTRE FOR THEORETICAL PHYSICS
34100 TRIESTE (ITALY) - P.O.B. 586 - MIRAMARE - STRADA COSTIERA 11 - TELEPHONE: 2240-1
CABLE: CENTRATOM - TELEX 460392-1

H4.SMR/210 - 24

SPRING COLLEGE ON PLASMA PHYSICS

(25 May - 19 June 1987)

FROZEN MAGNETIC FIELD CONDITION

B. Sonnerup

Thayer School of Engineering
Hanover, NH, USA

B. Sonnerup

Frozen Magnetic Field Condition

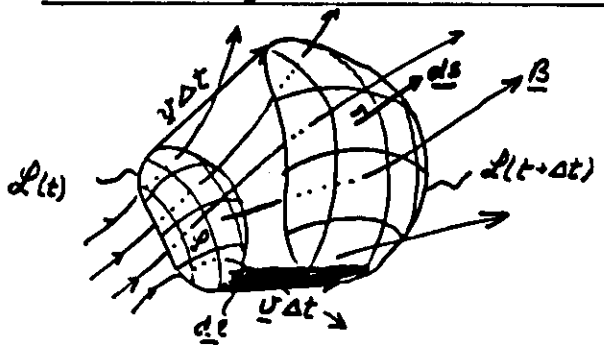

Loop $\mathcal{L}$ moves with veloc. $\underline{v}$

- $$\frac{D}{Dt}\int_{\mathcal{S}} \underline{B}\cdot d\underline{s} = \int_{\mathcal{S}} \frac{\partial \underline{B}}{\partial t}\cdot d\underline{s} + \frac{1}{\Delta t}\oint_{\mathcal{L}} (\underline{v}\Delta t \times d\underline{\ell})\cdot \underline{B}$$

$$\because \underline{\frac{D}{Dt}\int \underline{B}\cdot d\underline{s} = \int\left[\frac{\partial \underline{B}}{\partial t} - \nabla\times(\underline{v}\times\underline{B})\right]\cdot d\underline{s}}$$

- Ohm's Law: $\underline{j}/\sigma = (\underline{E} + \underline{v}\times\underline{B})$

$$\because \nabla\times \underline{j}/\sigma = -\frac{\partial \underline{B}}{\partial t} + \nabla\times(\underline{v}\times\underline{B})$$

$$\underline{\frac{D}{Dt}\int_{\mathcal{S}} \underline{B}\cdot d\underline{s} = -\oint_{\mathcal{L}} \frac{1}{\sigma}\underline{j}\cdot d\underline{\ell}} \quad \rightarrow 0 \text{ if } \sigma \rightarrow \infty,\ j \text{ finite, or if } j \rightarrow 0$$

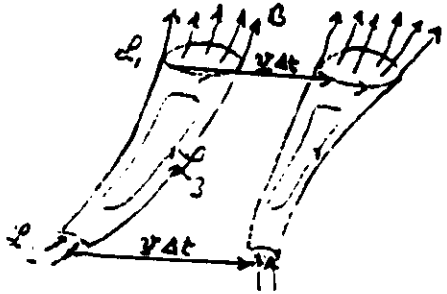

- Flux tubes frozen in fluid
- Field lines frozen in fluid.

Field line velocity or flux transport velocity:

$$\underline{E} + \underline{v}\times\underline{B} \simeq 0$$

$$\underline{v} = \underline{v}_\perp + \underline{v}_\parallel$$

$$\underline{v}_\perp = \underline{v}_\phi = \frac{\underline{E}\times\underline{B}}{B^2}$$

$\underline{v}_\phi$ moves points which were originally located on one field line in such a way that they remain located on a field line at later times:

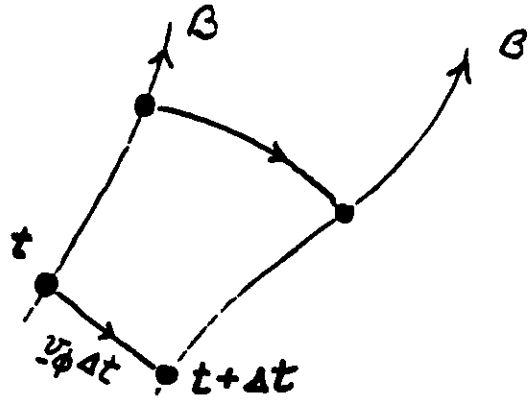

What does $\sigma \to \infty$ mean?

$$\underline{j} = \sigma(\underline{E} + \underline{v} \times \underline{B})$$

$$\underline{j} = \frac{1}{\mu_0} \nabla \times \underline{B} \simeq \frac{1}{\mu_0} \frac{B_0}{\ell}$$

When is the term $\underline{j}$ much less than $\sigma \underline{v} \times \underline{B}$ in magnitude?

$$|\underline{j}| / |\sigma \underline{v} \times \underline{B}| \simeq \frac{1}{\mu_0 \sigma v_0 \ell} \equiv \frac{1}{R_m} << 1$$

$R_m \equiv \mu_0 \sigma v_0 \ell$ is the <u>magnetic Reynolds #</u>

(Lundquist # $S \equiv \mu_0 \sigma v_A \ell$)

∴ Frozen condition requires $R_m >> 1$

Note that even if the overall length scale L of a problem is huge, as is often the case in cosmic plasma, the plasma may be capable of producing scale lengths ℓ such that R_m based on ℓ is of order one.

Current Sheet Formation $\sigma = \infty$

<u>Ex</u> Two plane dipoles in a very tenuous plasma: $\beta = 2\mu_0 p / B^2 << 1$. (Priest...)

$$\begin{cases} \text{Time } t=0: & B_{x0} - iB_{y0} = i d_0 \dfrac{4a_0 z}{(z^2 - a_0^2)^2} \\ \text{Time } t>0: & B_x - iB_y = i d \dfrac{4a_0^2}{\sqrt{a_0^2 + L^2}} \dfrac{\sqrt{z^2 + L^2}}{(z^2 - a_0^2)^2} \end{cases}$$

Flux cons. $\int_0^\infty B_{ox}\, dy = \int_L^\infty B_x\, dy$ gives relation between L/a_0 and d/d_0

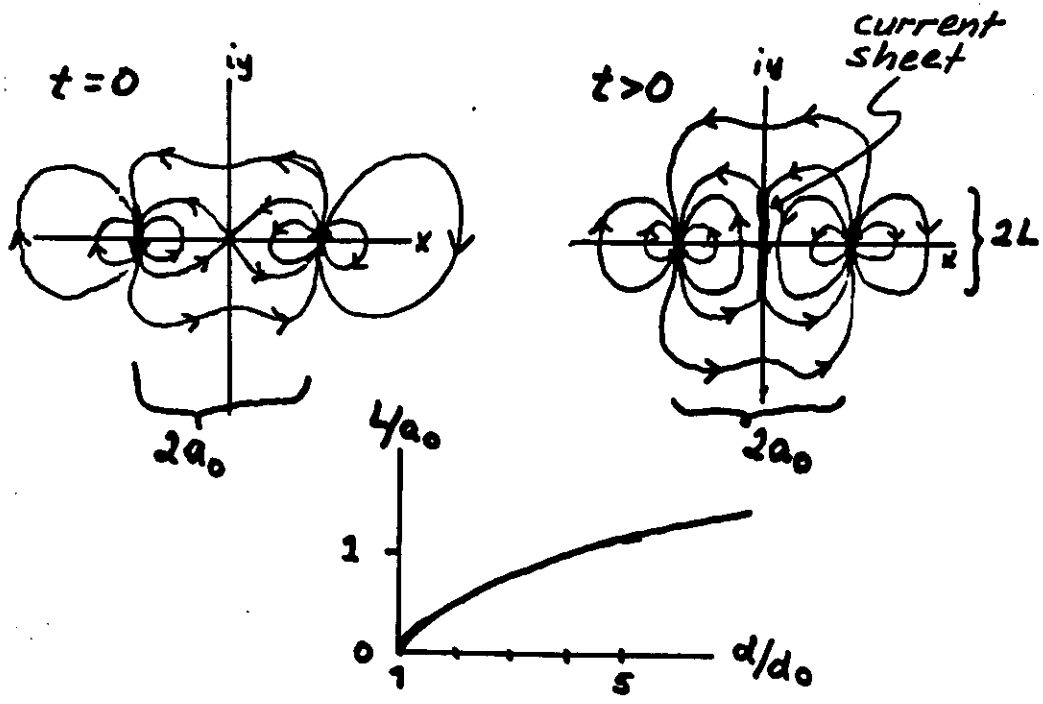

∵ Plasma has created a very small scale length (the thickness of the current sheet) so the frozen magnetic field condition may break down: reconnection may occur:

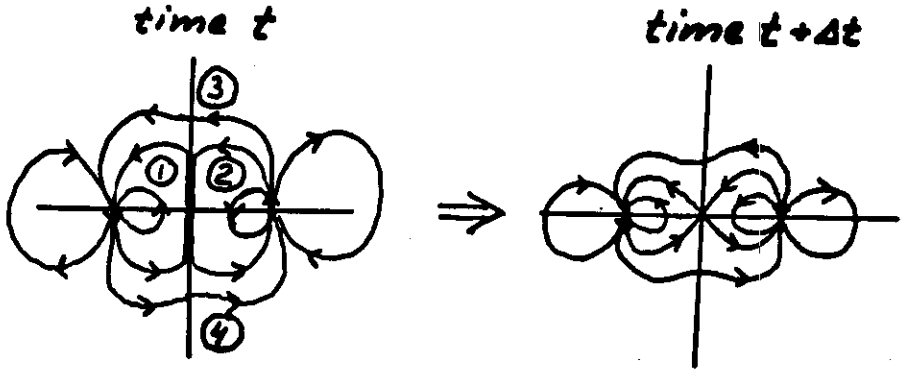

- "Spontaneous reconnection" returns the configuration to one of lower magnetic energy.
- Flux transfered from magnetic cells ① and ② to cells ③ and ④
- Magnetic energy converted to plasma kinetic energy and thermal energy.

- "Steady-state reconnection": flux transp. from cells ① and ② into ③ and ④ exactly balances flux addition into ① and ② as dipole strength increases w. time.

Definition of Reconnection

$v_{in} \sim \frac{E_r}{B_{in}}$

$v_{out} \sim \frac{E_r}{B_{out}}$

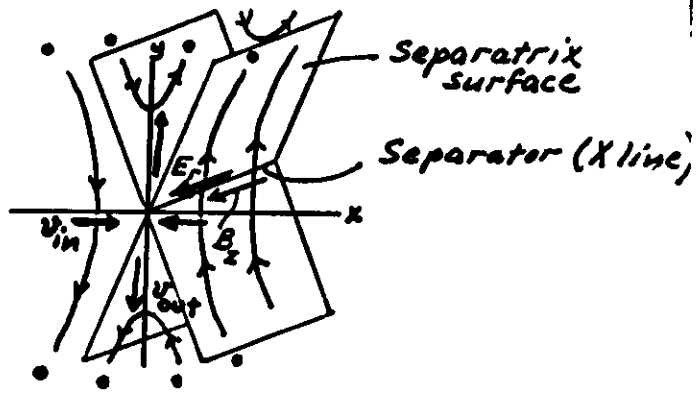

- A separatrix is a surface separating different magnetic cells.

- A separator is the line of intersection of a separatrix with itself or with another separatrix.

- Reconnection (merging) occurs when an electric field E_r is present along a separator.

- The reconnection rate is given by E_r. It is equal to the magnetic flux transported across unit length of separator/time

Comments on definition

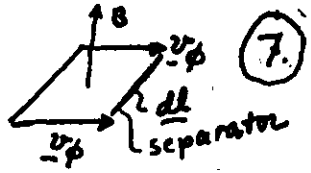

(7.)

- A magnetic field component B_z may be present along the separator
- Separator = X line = reconnection line = merging line (= neutral line = null line)
- Definition does not refer to "moving field lines" only to $\underline{E}$ and $\underline{B}$-topology.
- Definition emphasizes flux transport rather than plasma transport across a separatrix. (Reconnection may occur in a vacuum).

$$\underline{v}_\phi = \frac{\underline{E}\times\underline{B}}{B^2} = \text{flux transp. veloc}$$

$(\underline{E}\cdot\hat{\underline{B}} = 0)$ violated at separator

- Flux transported per unit time across length element dl of separator:

$$d\dot{\phi}_m = \underline{B}\cdot\{\underline{v}_\phi \times d\underline{l}\} \rightarrow \frac{d\dot{\phi}_m}{dl} = E_r$$

- Steady state reconnection rate is often written as $M_{A_1} = \frac{E_r}{v_{A_1} B_1}$
- Def. is local; E_r electrostatic or induced.

Sweet - Parker Model

(Parker 1963)

(8.)

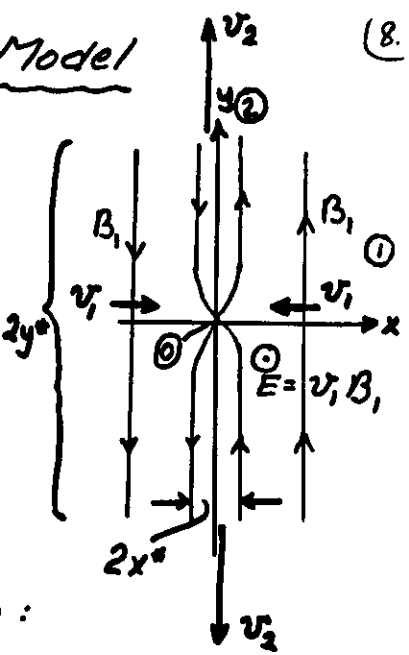

Four simple steps:

1. Bernoulli ⓪ - ②:

$$p_0 \cong p_1 + \frac{B_1^2}{2\mu_0} \cong p_2 + \frac{1}{2}\rho v_2^2 \quad (p_2 = p_1)$$

$$\because v_2 \cong B_1/\sqrt{\mu_0\rho} = v_{A_1}$$

2. Mass conservation:

$$y^* v_1 = x^* v_2$$

$$\because x^*/y^* = v_1/v_2 = v_1/v_{A_1} = M_{A_1}$$

3. Ohm's + Ampère's law:

$$j = \sigma E = \sigma v_1 B_1$$

$$j = B_1/\mu_0 x^* \qquad \because \underbrace{\mu_0 \sigma v_1 x^*}_{R_1} = 1$$

4. Eliminate x^*: $M_{A_1} = \frac{1}{\mu_0\sigma v_{A_1} y^*} = \frac{1}{\sqrt{R_m}}$

$R_m \gg 1$ so M_{A_1} is very small. — Lundquist #

Sweet-Parker with Viscosity

(W. Park et al Phys Fluids June 84)

Change Bernoulli to include work done by viscous forces. (viscosity)

$$p_1 + \frac{B_1^2}{2\mu_0} = p_1 + \frac{1}{2}\rho v_2^2 + \mu \frac{\bar{v}_y}{x^{*2}} y^*$$

Let $\bar{v}_y = v_2/2$ $\quad y^*/x^* = v_2/v_1$ *

Find $v_2 = v_{A_1} / \sqrt{1 + \frac{\nu}{v_1 x^*}}$ (ν ← kinematic viscosity, $\nu = \frac{\mu}{\rho}$)

From Ohm-Ampère as before:

$$\mu_0 \sigma v_1 x^* = 1 \quad ** \qquad \because v_2 = v_{A_1} / \sqrt{1 + \mu_0 \sigma \nu} \quad ***$$

Combine *, ** and *** to get

$$M_{A_1} \simeq \frac{1}{\sqrt{R_m}\,[1+\mu_0 \sigma \nu]^{1/4}}$$

Spitzer 1962 (transport ⊥ to strong B)

$$\mu_0 \sigma \nu = \frac{3\sqrt{2}}{40\pi} (T_e/T_i)^{1/2} (m_i/m_e)^{1/2} \beta_e$$

∵ Correction important when $\beta_e \geq O(1)$

Stagnation Point Flow

Resistive Field Annihilation

(Parker 1973, Sonnerup - Priest 1975)

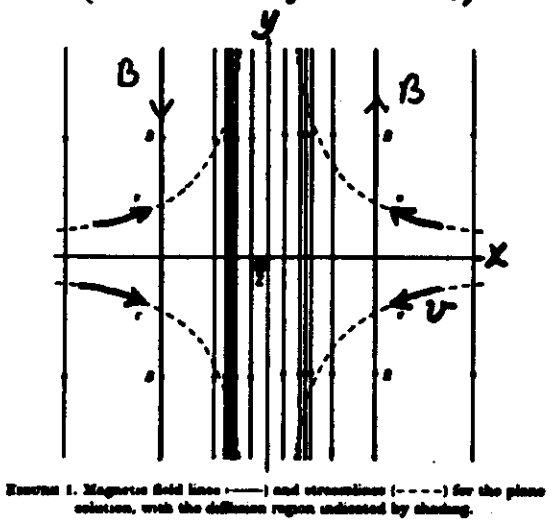

Figure 1. Magnetic field lines (——) and streamlines (- - - -) for the plane solution, with the diffusion region indicated by shading.

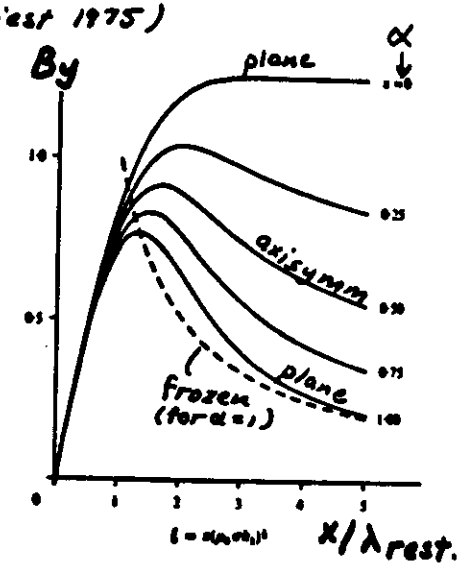

$$v_x = -k_1 x \qquad v_y = k_2 y \qquad v_z = k_3 z$$

$\nabla \cdot \underline{v} = 0$ ↙

$$k_1 = k_2 + k_3 \qquad \alpha = \frac{k_2}{k_1}$$

$$\lambda_{resistive} \equiv (\mu_0 \sigma k_1)^{-1/2}$$

- Inclusion of regular Newtonian viscosity leaves this flow unchanged
- Arbitrariness of M_{A_1} as a measure of the reconnection rate

Petschek Model

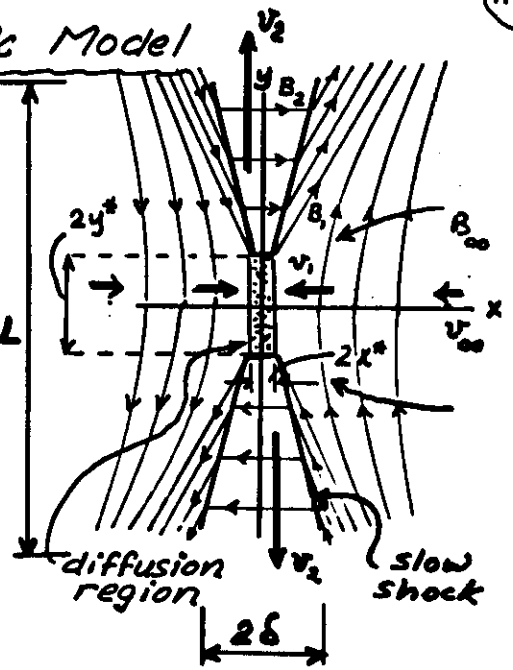

Outflow speed:

Mass $L v_1 = \delta v_2$

Flux $\delta B_1 = L B_2$

Tang. Mom. $\rho v_1 v_2 = \frac{B_1 B_2}{\mu_0}$

$\therefore v_2 = \frac{B_1}{\sqrt{\mu_0 \rho}}$

For very small flow rate:

$y^* \to L \quad x^* \to \delta$

no shocks; Sweet-Parker

As flow rate increases: v_2 ~ unchanged

δ increases

y^*, x^* decrease

x^*/y^* increases

- Max rate:

$$M_{A_\infty} = \left(\frac{v_\infty}{v_{A_\infty}}\right) \simeq \frac{\pi}{8 \ln\left(2 M_{A_\infty} R_{m_L}\right)} \sim 0.1$$

$(M_{A_1} = 1)$

- Fast mode expansion in inflow:

$v \uparrow \quad B \downarrow \quad \rho \downarrow \quad M_A \uparrow$ (Vasyliunas, 1975)

Similarity Model

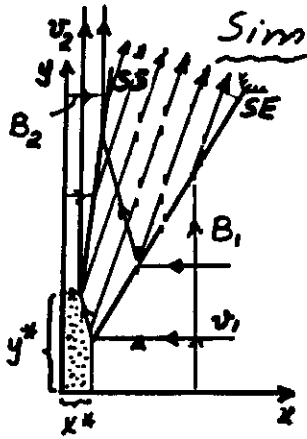

$\frac{v_1}{v_{A_1}} = 0.5$

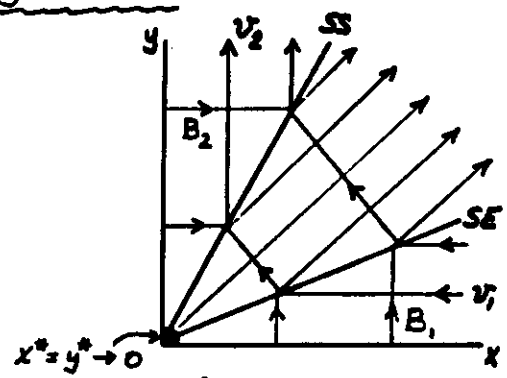

$\frac{v_1}{v_{A_1}} = \max = (1+\sqrt{2})$

$v_2 = v_1$

$B_2 = B_1$

- Outflow speed $v_2 = v_{A_1}(1+\sqrt{2})$ always.
- Max reconnection rate $M_{A_1} = \frac{v_1}{v_{A_1}} = 1+\sqrt{2}$

  Geometry is symmetric
- Slow mode expansion waves (SE) in inflow $B \uparrow \quad \rho \downarrow$
- SE turn to expansion fans centered at external "corners" for compr. case
- Another possibility: add appropriate B_z (and v_2) so that $|B| = \text{const}$. Then all waves are Alfvén waves (RD's)

(Hameiri, 1978)

Asymmetric Petschek Model

(Magnetopause reconnection)

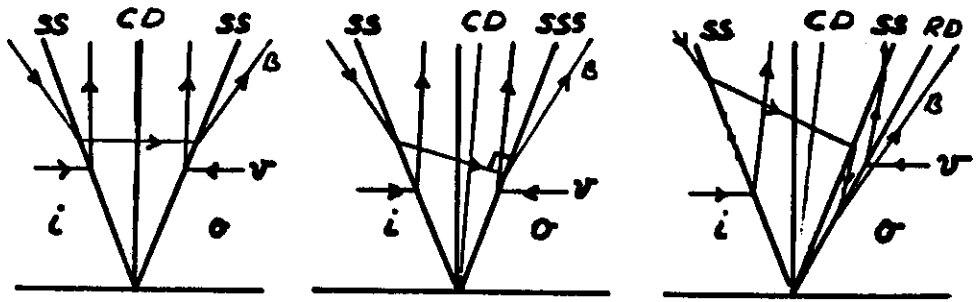

$\rho_i = \rho_o$
$T_i = T_o$

$\rho_i < \rho_o$
switch-off
shock at right

$\rho_i \ll \rho_o$

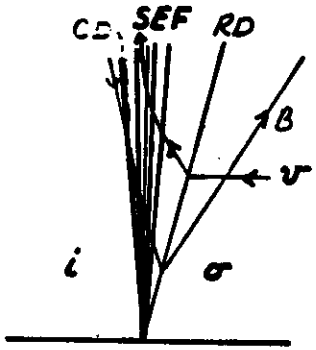

SS = Slow shock
SSS = Slow switch-off shock
SEF = Slow expansion fan
RD = Rotational discont.
CD = Contact discont.

$\rho_i = 0$, $P_i = 0$

(Levy-Petschek-Siscoe 1964
Petschek and Thorne 1967
Yang-Sonnerup 1976
Heyn and Biernat 1985)

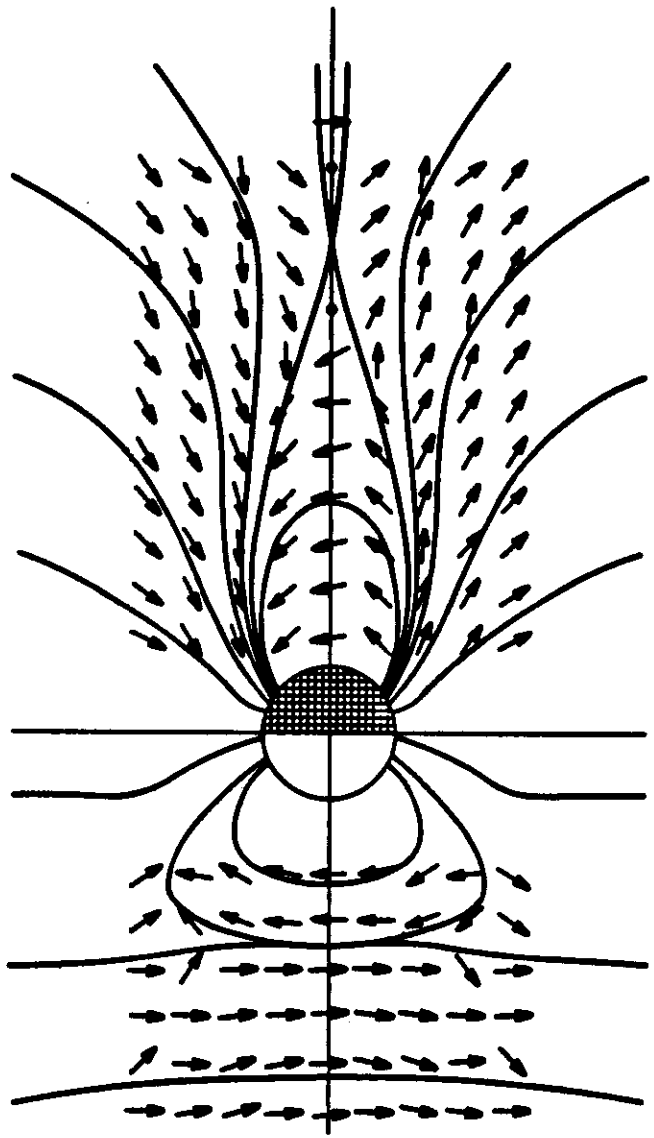

Fig. 14 Typical magnetic field map of the UCR T-1 magnetosphere for a southward IMF at Alfvén Mach number 2.5 during the fast plasma phase. (From Ream and Bratenahl, 1982a.)

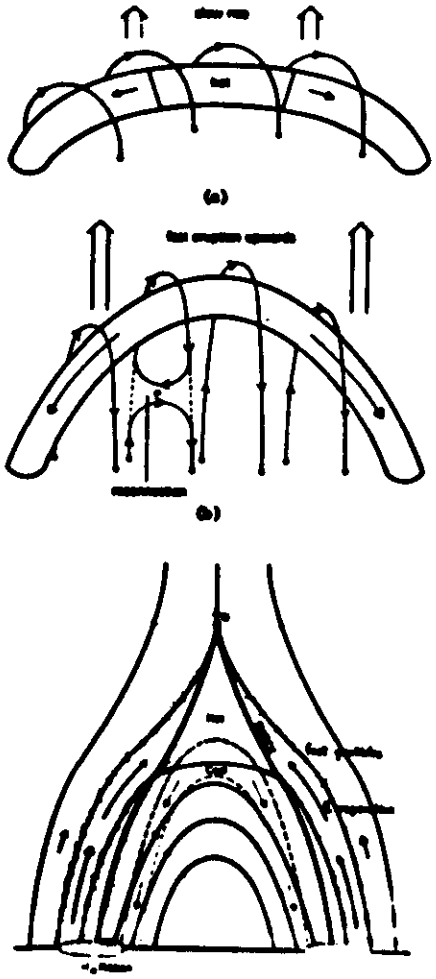

Fig. 12. The overall behaviour of a large flare: (a) preflare phase, (b) rise phase, (c) a section across the arcade during the main phase.

Priest 1983

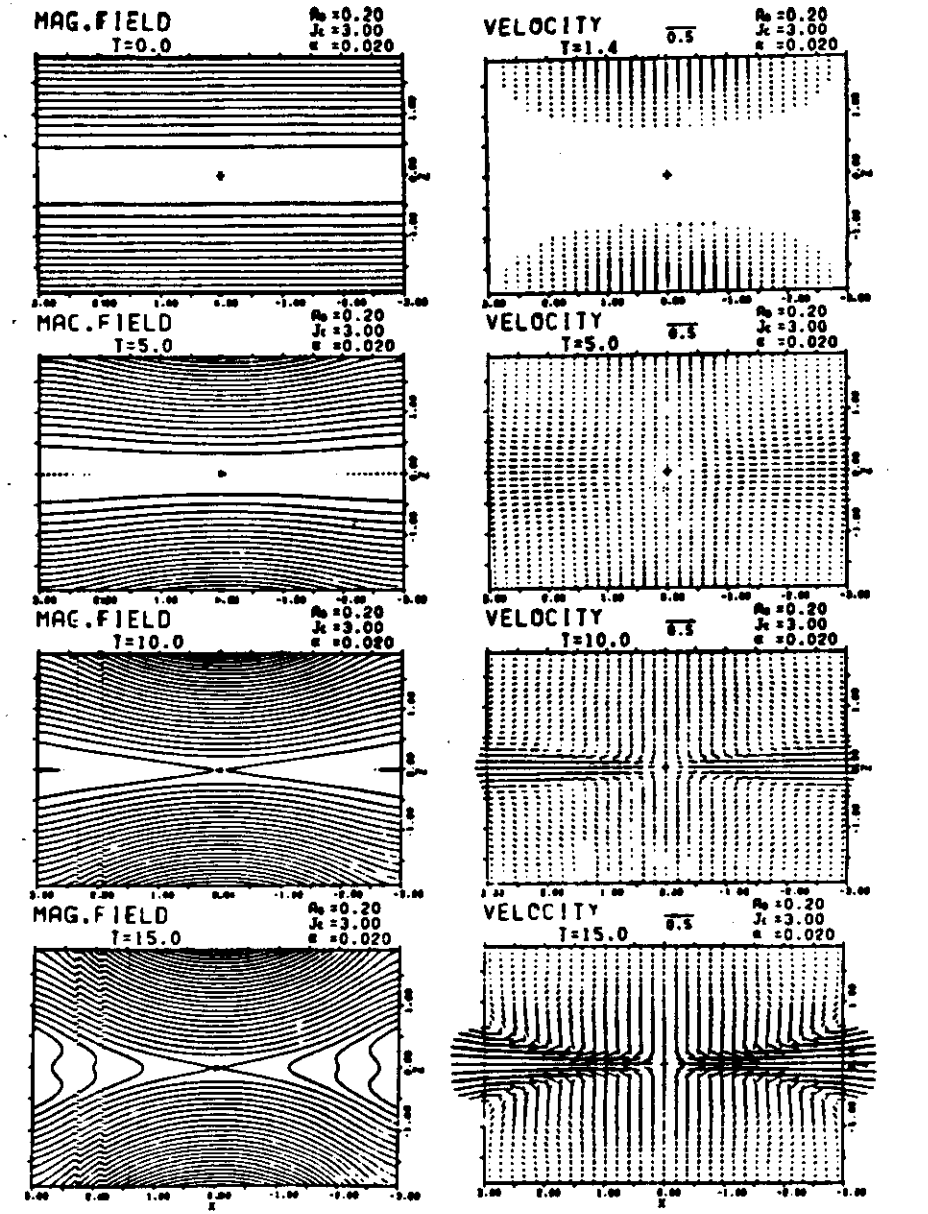

FIG. 1. Computer plots of reconnecting magnetic field lines, or equivector potential lines (left) and plasma flow vectors (right). Note evidence of fast mode expansion in the upstream region, i.e., cusp-like flow direction change, in the bottom right panel (T=15.0).

Sato-Hayashi Phys Fluids June 1979

Reconnection in Tokamak (m=1 flip)

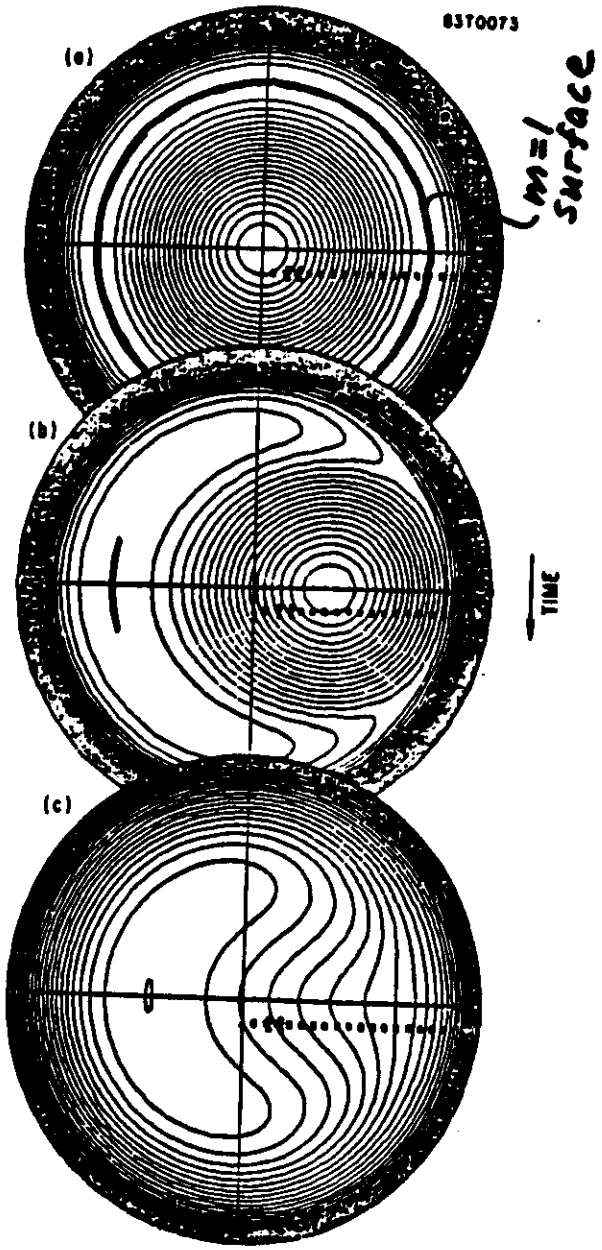

W. Park (1983)

Diffusion Region: Two-fluid effects

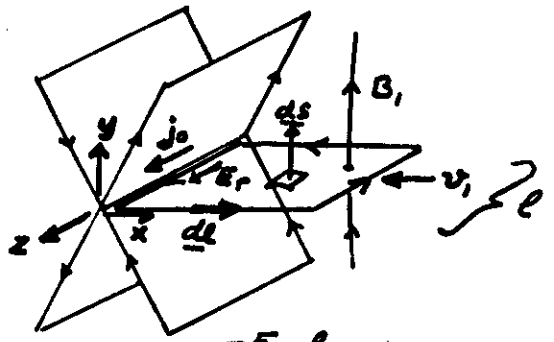

$$-E_r\, l$$

$$\frac{D}{Dt}\int \underline{B}\cdot d\underline{s} = -\oint(\underline{E}+\underline{v}\times\underline{B})\cdot d\underline{l} = \frac{1}{n_0 e}\left(\frac{\partial B_z}{\partial x}+\frac{\partial B_z}{\partial y}\right)$$

$$= -\oint \frac{\underline{j}}{G}\cdot d\underline{l} \;(-j_0 l/G_0) - \oint \frac{\underline{j}\times\underline{B}}{ne}\cdot d\underline{l}\;(0) + \oint \frac{1}{ne}\nabla\cdot\underline{P}_e\cdot d\underline{l}$$

$$- \oint \frac{m_e}{ne^2}\left(\frac{\partial \underline{j}}{\partial t} + \nabla\cdot(\underline{j}\underline{v} + \underline{v}\underline{j})\right)\cdot d\underline{l} \quad (0 \text{ (plane case)})$$

- Contribution to line integrals only along separator
- Only $G_0 < \infty$ or FLR effects in electron pressure tensor can unfreeze the flux
- Scale size from FLR is $\lambda_e = \sqrt{\frac{m_e}{\mu_0 n e^2}}$ (x velocity of electrons is brought to zero over this distance. What about ions?)

Stagnation-Point Flow

Electron inertia effects

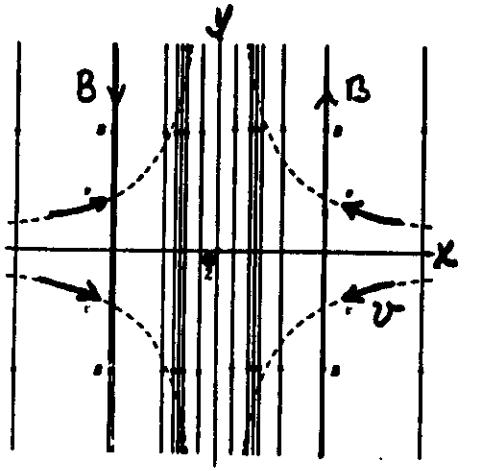

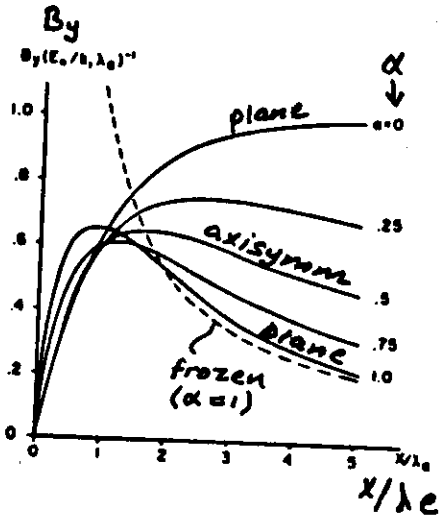

FIGURE 1. Magnetic field lines (——) and streamlines (- - - -) for the plane solution, with the diffusion region indicated by shading.

$$\left.\begin{aligned} v_x &= -k_1 x \\ v_y &= k_2 y \\ v_z &= k_3 z \end{aligned}\right\} \qquad k_1 = k_2 + k_3 \qquad \alpha = k_2/k_1$$

$$\lambda_e = \sqrt{\frac{m_e}{\mu_0 n e^2}}$$

FLR effects not included in electron pressure tensor.

Hall Term $\frac{1}{ne}\underline{j}\times\underline{B}$

Two possibilities:

a) $\underline{\nabla}\times\left(\frac{1}{ne}\underline{j}\times\underline{B}\right)=0$

If boundary conditions permit, Hall term may be cancelled completely by Hall electric field E_H. Then $x^* \sim \lambda_e$ or R_{Le} (for $\sigma=\infty$)

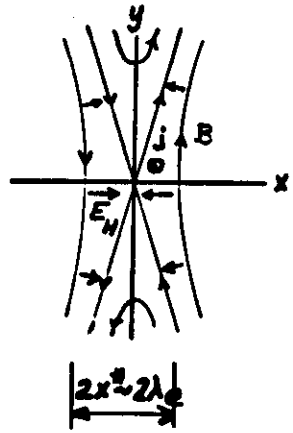

b) Otherwise ions will be brought to a halt over a distance $\sim\lambda_i$ or R_{Li} and electrons over λ_e or R_{Le}. The result will be Hall current loops over distance λ_i or R_{Li}

$$\frac{D}{Dt}\int\underline{B}\cdot\underline{da} = -\oint\frac{1}{ne}(\underline{j}_H\times\underline{B})\cdot\underline{dl}$$

Hall current unfreezes the ions!

$x^* \sim \lambda_i$ or R_{Li}

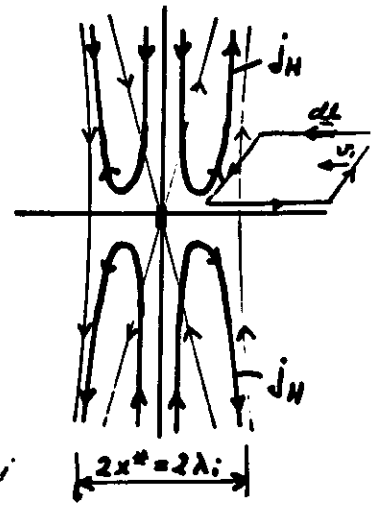

2. THE FROZEN MAGNETIC FIELD CONDITION

2.1 Mathematical Background

Consider a loop $\mathcal{L}$ which bounds an open surface $\mathcal{S}$, located in a magnetic field $\underline{B}(\underline{r},t)$, as shown in Figure 1. The magnetic flux through this surface is

$$\phi_m = \int_{\mathcal{S}} \underline{B}\cdot d\underline{s} \qquad (1)$$

and because $\nabla\cdot\underline{B} = 0$, the same magnetic flux is obtained for any surface bounded by $\mathcal{L}$. We shall take advantage of this freedom in the choice of $\mathcal{S}$ later on.

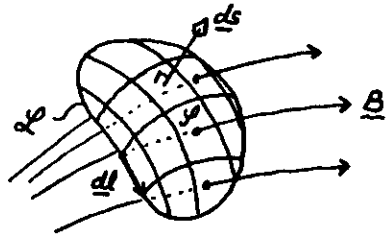

Fig. 1

Now imagine that the loop is moved by some arbitrary velocity field $\underline{V}(\underline{r},t)$ (which, at this point in the discussion, is not tied in any way to the physical motion of the plasma in which $\underline{B}$ may be imbedded). In other words, each length element $d\underline{\ell}$ of the loop moves at its own velocity, the result being that the loop as a whole may be displaced while, at the same time, it is deformed. We want to calculate $D\phi_m/Dt$, the rate of change of the magnetic flux which occurs, both as a result of this motion and deformation and as a result of the time variability of $\underline{B}$ itself. The rates produced by these two effects can be calculated separately and then added.

Consider just the rate of change, $(d\phi_m/dt)_1$, produced by the temporal variation of $\underline{B}$. This rate is evaluated with the loop and surface in a

fixed position and is given by

$$\left(\frac{d\phi_m}{dt}\right)_1 = \frac{d}{dt}\int_{\mathcal{S}} \underline{B}\cdot d\underline{s} = \int_{\mathcal{S}} \frac{\partial \underline{B}}{\partial t}\cdot d\underline{s} \qquad (2)$$

Note that the assumption that the surface $\mathcal{S}$ is fixed means that the limits of the surface integral are independent of time. It is for this reason that the time derivative may be moved inside the integral sign. Since $\underline{B}$ is a function of space as well as time, while the integral is a function of time only, the time derivative must be written as a partial derivative when it is placed inside the integral sign.

We turn now to $(d\phi_m/dt)_2$, the rate of change of magnetic flux produced by the motion and deformation of the loop. This rate is to be evaluated under the assumption that $\underline{B}$ does not change with time. Since ϕ_m is the same for any surface, $\mathcal{S}$ bounded by $\mathcal{L}$ we now choose a surface such that the vector $d\underline{\ell}\times\underline{V}dt$ is normal to the surface at each point along $\mathcal{L}$. Furthermore, as shown in Figure 2, the magnitude of this vector is the area swept out by the length element $d\underline{\ell}$ in the time increment dt. For the element shown in the

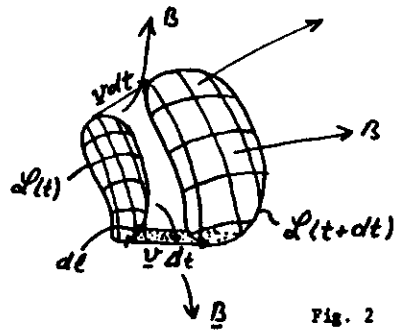

Fig. 2

figure the motion leads to a change in magnetic flux in the amount $-\underline{B}\cdot(d\underline{\ell}\times\underline{V}dt)$, the negative sign indicating that, with the direction of $\underline{V}$ shown, the flux decreases. By integration around the loop, the net rate of change of the flux

due to the motion and deformation of the loop becomes

$$\left(\frac{d\phi_m}{dt}\right)_2 = -\oint_{\mathcal{L}} \underline{B}\cdot(\underline{dl}\times\underline{V}) \tag{3}$$

which, by cyclic permutation of the vectors in the scalar triple product and by subsequent use of Stokes' theorem may be written

$$\left(\frac{d\phi_m}{dt}\right)_2 = -\oint_{\mathcal{L}} \underline{dl}\cdot(\underline{V}\times\underline{B}) = -\int_{\mathcal{S}} \underline{\nabla}\times(\underline{V}\times\underline{B})\cdot\underline{ds} \tag{4}$$

We may now add the rates in (2) and (4) to obtain the total rate of change of the magnetic flux:

$$\frac{D\phi_m}{Dt} = \left(\frac{d\phi_m}{dt}\right)_1 + \left(\frac{d\phi_m}{dt}\right)_2 = -\int_{\mathcal{S}}\left[\frac{\partial\underline{B}}{\partial t} - \underline{\nabla}\times(\underline{V}\times\underline{B})\right]\cdot\underline{ds} \tag{5}$$

This result is sometimes referred to as the "changing flux theorem." In reality it is not restricted to the magnetic field $\underline{B}$ but is valid for any divergence-free vector field. In ordinary hydrodynamics for example, $\underline{B}$ is replaced by the velocity vector, $\underline{\Omega}$, and the equation then forms the basis for Lord Kelvin's theorem of frozen vorticity in an ideal fluid.

For our purposes, we may now replace $\partial\underline{B}/\partial t$ by $-\underline{\nabla}\times\underline{E}$ in accordance with Faraday's law so that

$$\frac{D\phi_m}{Dt} = -\int \underline{\nabla}\times[\underline{E}+\underline{V}\times\underline{B}]\cdot\underline{ds} = -\oint [\underline{E}+\underline{V}\times\underline{B}]\cdot\underline{dl} \tag{6}$$

where the last member again follows from Stokes' theorem. For nonrelativistic motion, the quantity $\underline{E}+\underline{V}\times\underline{B} \equiv \underline{E}''$ represents the electric field in a frame of reference moving with the local velocity $\underline{V}$ relative to the laboratory frame (in which the electric field is $\underline{E}$). Thus we may finally write

$$\frac{D\phi_m}{Dt} = -\oint \underline{E}''\cdot\underline{dl} \tag{7}$$

If $\underline{E}'' = 0$ or, more generally, if $\underline{E}'' = -\underline{\nabla}\phi(\underline{r},t)$ where ϕ is an arbitrary potential, we find the frozen-flux theorem:

$$\frac{D\phi_m}{Dt} = 0 \tag{8}$$

This theorem, expressed by Equation (8), states that the magnetic flux through the loop remains frozen at its initial value as the loop moves and deforms in a generally nonsteady manner in a magnetic field that is also time variable, in general.

In Figure 3, we show two loops, $\mathcal{L}_1(t_0)$ and $\mathcal{L}_2(t_0)$, which initially (i.e., at time $t = t_0$), are linked by the same bundle of magnetic field lines, defining a magnetic flux tube. We also imagine a large number of small loops, $\mathcal{L}_3(t_1)$, $\mathcal{L}_4(t_0)$,...., all located on the surface of that tube and therefore each linking zero magnetic flux. As these loops are moved to new positions by the velocity field $\underline{V}(\underline{r}, t)$, at the same time being deformed in various ways, the frozen flux theorem (8), if valid, would indicate that at any later time each loop still links the same flux as it did initially. In other words, the loops $\mathcal{L}_3(t)$, $\mathcal{L}_4(t)$,.... are all located on the surface of a flux tube at any later time t and the two loops $\mathcal{L}_1(t)$ and $\mathcal{L}_2(t)$ still link the same amount of flux as they did initially. Thus is appears as if the entire original flux tube has been moved with the velocity field $\underline{V}(\underline{r},t)$,

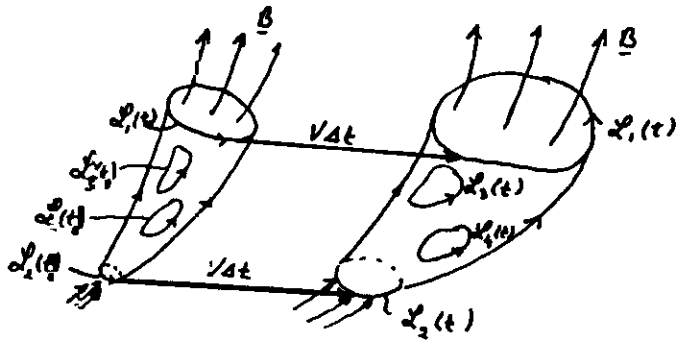

Fig. 3

undergoing various deformations in the process. This is one possible way of interpreting the implications of Equation (8). Furthermore, if the cross section of the flux tube is made vanishingly small, it then appears as if the individual magnetic field lines themselves are moved by the velocity field $\underline{V}(\underline{r},t)$, as illustrated in Figure 4. In this manner, the frozen-flux theorem is seen to be equivalent to a frozen-field line condition.

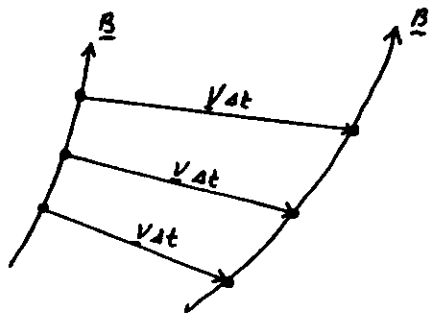

Fig. 4

We may ask in what circumstances, i.e., for what fields $\underline{E}$ and $\underline{B}$, it is possible to find a velocity field $\underline{V}$, such that

$$\underline{E}' = \underline{E} + \underline{V}\times\underline{B} = -\underline{\nabla}\phi \tag{9}$$

which is the basic requirement for the frozen flux theorem to be valid. As is seen from (9), such a velocity can be found, provided the electric field component, if any, along $\underline{B}$ can be expressed as

$$\underline{E}\cdot\hat{\underline{B}} = -\hat{\underline{B}}\cdot\underline{\nabla}\phi \tag{10}$$

We may then write

$$\underline{V} = (\underline{E}+\underline{\nabla}\phi)\times\underline{B}/B^2 + V_{\parallel}(\underline{r},t)\hat{\underline{B}} \tag{11}$$

where $V_{\parallel}(\underline{r},t)$ is an arbitrary velocity component along $\underline{B}$. The perpendicular component

$$\underline{V}_{\perp} = (\underline{E}+\underline{\nabla}\phi)\times\underline{B}/B^2 \tag{12}$$

is referred to as the "field-line velocity" or the "flux-transport" velocity.

Objections are sometimes raised to the concept of moving field lines and it is clear that, unless the condition (10) is satisfied, such objections are valid. Even when (10) is satisfied it is a matter of personal taste whether or not one wants to think about phenomena in terms of moving field lines. Those who do not like this concept may simply think of the velocity $\underline{V}_{\perp}$ as having the property of moving a set of points originally located on a field line in such a manner that at any later time they remain located on a field line. There is no need to conclude that it is one and the same field line that has moved. However, in this paper we find it convenient to adopt the concept of moving field lines. For example, consider the vacuum electromagnetic field shown in Figure 5. It consists of a constant electric field $E_0\hat{\underline{z}}$ at right angles to a hyperbolic magnetic field, $\underline{B} = k(y\hat{\underline{x}}+x\hat{\underline{y}})$, where k is a constant, and it satisfies the condition (10) with $\underline{\nabla}\phi \equiv 0$. We shall think of the magnetic field lines in this configuration as moving with $\underline{V}_{\perp}$ in the manner shown, the result being the transport of magnetic flux across the separatrix lines ($y = \pm x$) from cells ① and ② into cells ③ and ④ with accompanying reconnection of magnetic field lines from cells ① and ② as they reach the X-type null in the field at the origin.

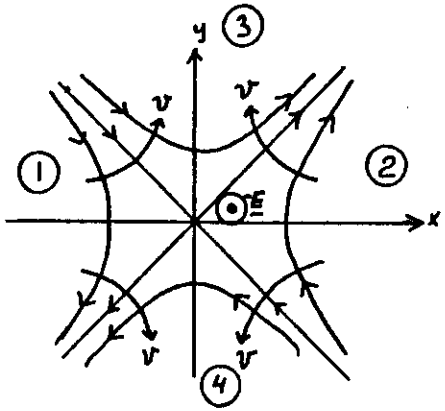

Fig. 5

As an illustration of the role played by the term $-\nabla\phi$ in (12), consider the case of an idealized plasma discontinuity such as a shock or rotational discontinuity which has uniform (but different) magnetic fields on its two sides and a nonvanishing magnetic field component normal to the discontinuity, as illustrated in Figure 6. In the so-called deHoffmann-Teller frame of reference, the discontinuity is stationary and has zero electric fields on both sides. However, within the structure of the discontinuity itself an electric field $\underline{E} = -\nabla\phi = -\hat{n}(\partial\phi/\partial n)$ normal to the layer is usually present. In this case too, the condition (10) is satisfied and the field line velocity $\underline{V}_\perp$ given by (12) is identically zero, not only on the two sides of the layer where $\underline{E} \equiv 0$ but also in its interior where $\underline{E} = -\nabla\phi$. Thus the field lines may be thought of as being entirely at rest in the de Hoffmann-Teller frame.

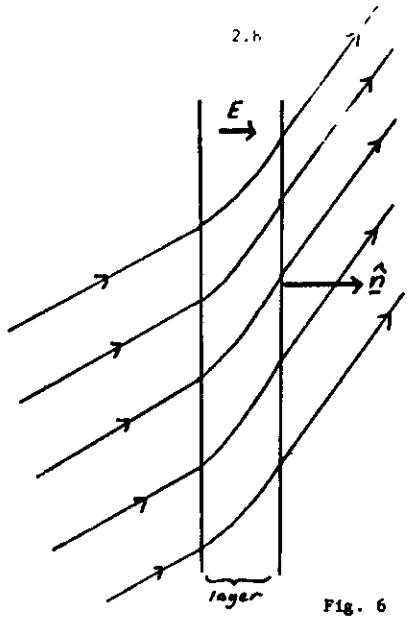

Fig. 6

Finally, we emphasize again that up to this point no connection has been made between the field-line velocity $\underline{V}_\perp$ and the perpendicular component of the actual plasma velocity, $\underline{v}_\perp$ assuming that the electromagnetic fields we have discussed occur in an electrically conducting fluid. In the next section, we shall argue that they are sometimes but by no means always the same. For example, in the case of the discontinuity shown in Figure 6, the two perpendicular velocities are the same and equal to zero on the two sides of the layer. However, in its interior the field line velocity is zero while the plasma velocity component perpendicular to $\underline{B}$ is not.

2.2 Ohm's Law

The simplest version of Ohm's Law in a moving fluid states that the electric current density, $\underline{j}$, is proportional to the electric field, $\underline{E}'$, measured in the frame of reference moving with the fluid velocity $\underline{v}$. In other words,

$$\underline{j} = \sigma \underline{E}' = \sigma(\underline{E} + \underline{v} \times \underline{B}) \tag{13}$$

where σ is the electrical conductivity (mho/m). If we now let $\underline{V} = \underline{v}$ (and therefore $\underline{E}'' = \underline{E}'$) in (7) we arrive at the result

$$\frac{D\phi_m}{Dt} = -\oint_{\mathcal{L}} \frac{j}{\sigma} \underline{j} \cdot d\underline{l} \tag{14}$$

The magnetic flux is seen to become frozen into the moving fluid in the limit $\sigma \to \infty$. It is also frozen in regions where $\underline{j} = 0$, and it tends to become unfrozen in regions where $\underline{j}$ is large.

In practice, the frozen flux condition is almost never precisely satisfied. A useful criterion by which one can judge how well the flux is frozen is obtained by comparing the term $\sigma \underline{v} \times \underline{B}$ to the term $\underline{j}$ in Ohm's Law. If we denote by v_o, B_o and L the characteristic values of velocity, magnetic field, and scale length in a fluid flow, and if we estimate $\underline{j}$ as $B_o/\mu_o L$ in accordance with Ampère's law, we find

$$\frac{|\sigma \underline{v} \times \underline{B}|}{|\underline{j}|} = \frac{\sigma v_o B_o}{B_o/L\mu_o} = \mu_o \sigma v_o L$$

The dimensionless group $R_m = \mu_o \sigma v_o L$ is called the magnetic Reynolds number. (When the Alfvén speed $v_{Ao} = B_o/\sqrt{\mu\rho}$ is used instead of v_o, the so-called Lundquist number, $S \equiv \mu_o \sigma v_{Ao} L$, is obtained.) If R_m is large, as is often the case in cosmic applications, on account of large values of L and v_o, then the frozen magnetic field condition holds to a good approximation. However,

note that even if the overall scale of a problem is large, the plasma geometry may, and often does, rearrange itself in such a way that narrow regions of high current density are formed. The R_m value based on the thickness ℓ of such layers rather than on the overall scale L may then become of order unity. In other words, the plasma finds a way to break the frozen flux condition locally. This is what is believed to happen in the vicinity of the X line of a reconnection configuration. It is useful to define a resistive length $\lambda_r \equiv (\mu_o \sigma v_o)^{-1}$ such that the magnetic Reynolds number based on λ_r is equal to unity.

Figure 7 shows a loop $\mathcal{L}$ = ABCD in the inflow region of a steady-state, two-dimensional reconnection configuration where the flow is associated with a uniform electric field $\underline{E}_o$. The segment AB of the loop where the

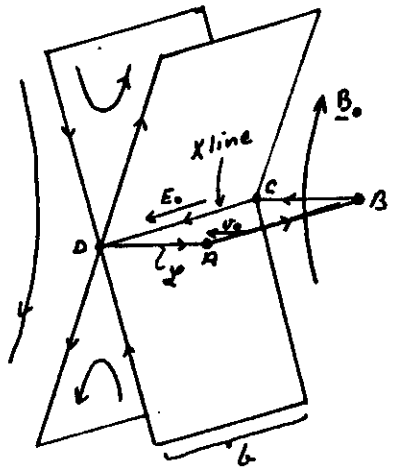

Fig. 7

magnetic field is B_o and where the current density is negligibly small is being carried towards the origin with speed v_o. The electric field is given by $E_o = v_o B_o$. The segment CD of the loop is located along the X line and therefore is stationary. Thus the area bounded by $\mathcal{C}$ decreases with time and the associated rate of change of magnetic flux in the loop is

$$\frac{D\phi}{Dt} = - v_o B_o b \tag{15}$$

where b is the length of the segment AB. The magnetic flux does not escape across AB because j=0 so that the frozen field condition holds there. Instead it can be considered as leaking across the X line where $\underline{j} = \sigma \underline{E}_o$ so that

$$- \oint \frac{1}{\sigma} \underline{j} \cdot d\underline{\ell} = - E_o b \tag{16}$$

We conclude that the amount of flux reconnected per unit length of the X line is simply $E_o = v_o B_o$. Thus E_o is a measure of the reconnection rate. A nondimensional expression for this rate is the Alfvén number

$$M_A \equiv \frac{v_o}{v_{Ao}} = \frac{E_o}{B_o v_{Ao}} \tag{17}$$

2.3 Generalized Ohm's Law

In a collisionless or nearly collisionless plasma, the simple form of Ohm's law used in the previous section is not always adequate. For this reason we now introduce a generalized version of Ohm's law which is valid in a plasma consisting of electrons (subscript e) of charge -e, and one kind of ions (subscript i) of charge Ze. The momentum equations for these two species are

$$n_i m_i \left(\frac{\partial \underline{v}_i}{\partial t} + \underline{v}_i \cdot \underline{\nabla} \underline{v}_i \right) = - \underline{\nabla} \cdot \underline{\underline{P}}_i + n_i Ze(\underline{E} + \underline{v}_i \times \underline{B}) - n_i m_i (\underline{v}_i - \underline{v}_e)/\tau_{ie} \tag{18}$$

$$n_e m_e \left(\frac{\partial \underline{v}_e}{\partial t} - \underline{v}_e \cdot \underline{\nabla} \underline{v}_e \right) = - \underline{\nabla} \cdot \underline{\underline{P}}_e - n_e e(\underline{E} + \underline{v}_e \times \underline{B}) - n_e m_e (\underline{v}_e - \underline{v}_i)/\tau_{ei} \tag{19}$$

where $\underline{\underline{P}}_i$ and $\underline{\underline{P}}_e$ are the stress tensors. By adding the two equations, making use of the condition of charge quasineutrality, $n_i Z = n_e$, as well as the definition of the current density, $\underline{j} = (n_i Z e \underline{v}_i - n_e e \underline{v}_e)$, the relation $n_i m_i / \tau_{ie} = n_e m_e / \tau_{ei}$ between the collision times τ_{ie} and τ_{ei}, and by neglecting m_e/m_i compared to unity one obtains the total momentum equation

$$\rho \left(\frac{\partial \underline{v}}{\partial t} + \underline{v} \cdot \underline{\nabla} \underline{v} \right) = - \underline{\nabla} \cdot \underline{\underline{P}} + \underline{j} \times \underline{B} \tag{20}$$

where $\rho = n_i m_i$, $\underline{v} = \underline{v}_i$ and $\underline{\underline{P}} = \underline{\underline{P}}_i + \underline{\underline{P}}_e$. If Equation (18) is multiplied by Ze/n_i and (19) by e/m_e and the latter is subtracted from the former, then neglecting terms of order m_e/m_i, we obtain

$$\frac{\partial \underline{j}}{\partial t} + \underline{\nabla} \cdot (\underline{j} \underline{v} + \underline{v} \underline{j}) = \frac{e}{m_e} \underline{\nabla} \cdot \underline{\underline{P}}_e + \frac{n_e e^2}{m_e} (\underline{E} + \underline{v}_e \times \underline{B}) - \underline{j} \frac{1}{\tau_{ei}} \tag{21}$$

i.e., noting that $\underline{v}_e = \underline{v} - \underline{j}/n_e e$

$$\underline{E} + \underline{v} \times \underline{B} = \underline{j}/\sigma + \frac{1}{n_e e} \underline{j} \times \underline{B} - \frac{1}{n_e e} \underline{\nabla} \cdot \underline{\underline{P}}_e + \frac{m_e}{n_e e^2} \left[\frac{\partial \underline{j}}{\partial t} + \underline{\nabla} \cdot (\underline{j} \underline{v} + \underline{v} \underline{j}) \right] \tag{22}$$

where $\sigma = n_e e^2 \tau_{ei}/m_e$ is the conductivity.

Equation (22) is the generalized Ohm's law. In addition to the terms $(\underline{E} + \underline{v} \times \underline{B})$ and $\underline{j}/\sigma$ which already appeared in the simple Ohm's law (Eq. 13), we have the following new terms: the Hall term $\underline{j} \times \underline{B}/n_e e$, the electron pressure term $(\underline{\nabla} \cdot \underline{\underline{P}}_e)/n_e e$ and the electron inertia term $m_e \left[\frac{\partial \underline{j}}{\partial t} + \nabla \cdot (\underline{j} \underline{v} + \underline{v} \underline{j}) \right] / n_e e^2$.

The ratio of the various terms on the right-hand side of Eq. (22) to the term $\underline{v} \times \underline{B}$ on the left may be estimated by use of a characteristic spatial scale L and temporal scale T_o and by assuming the characteristic

velocity to be of the order of the Alfvén speed:

$$\frac{|\underline{j}/\sigma|}{|\underline{v}\times\underline{B}|} \sim \frac{\lambda_r}{L} \tag{23}$$

$$\frac{|\underline{j}\times\underline{B}/n_e e|}{|\underline{v}\times\underline{B}|} \sim \frac{\lambda_i}{L} \;;\; \frac{R_{Li}}{L} \;;\left(\frac{R_{Li}}{L}\right)^2 \tag{24}$$

$$\frac{|\nabla\cdot\underline{P}_e/n_e e|}{|\underline{v}\times\underline{B}|} \sim \frac{R_{Le}}{L} \;;\left(\frac{R_{Le}}{L}\right)^2 \tag{25}$$

$$\frac{\left|\frac{m_e}{n_e e^2}\frac{\partial \underline{j}}{\partial t}\right|}{|\underline{v}\times\underline{B}|} \sim \frac{\lambda_e}{L}\frac{\lambda_e}{v_o T_o} \tag{26}$$

$$\frac{\left|\frac{m_e}{n_e e^2}\nabla\cdot(\underline{j}\underline{v}+\underline{v}\underline{j})\right|}{|\underline{v}\times\underline{B}|} \sim \frac{\lambda_e^2}{L^2} \tag{27}$$

where λ_r, λ_i, and λ_e are the resistive length, the ion inertial length and the electron inertial length, respectively, defined by

$$\lambda_r = 1/(\mu_o \sigma v_o) \tag{28}$$

$$\lambda_i = \sqrt{m_i/\mu_o n_i Z^2 e^2} \tag{29}$$

$$\lambda_e = \sqrt{m_e/\mu_o n_e e^2} \tag{30}$$

Also, R_{Li} and R_{Le} are the ion and electron gyroradii. Note that the estimates $(R_{Li}/L)^2$ and $(R_{Le}/L)^2$ in (24) and (25) come from the collisionless off-diagonal finite-Larmor-radius (FLR) terms in the ion and electron stress tensors.

The internal length scales λ_r, λ_i, λ_e, R_{Li}, and R_{Le} of the plasma can be used to estimate in what circumstances the various terms on the right-hand side of the generalized Ohm's law (22) may become important. All terms are negligible when L is much greater than all the internal plasma scales. Note that the inertial length and the gyroradius are comparable when the particle kinetic pressure and the magnetic pressure are comparable. The electron scale lengths are always much smaller than the ion ones. Typical values at the earth's magnetopause are $\lambda_e \sim 1$ km, $\lambda_i \sim 50$ km. The relative size of λ_r and λ_i, say, depends on the conductivity. For sufficiently large electrical conductivity, σ, we find $\lambda_r \ll \lambda_i$. For sufficiently small σ, the inequality reverses so that $\lambda_r \gg \lambda_i$.

The electron-ion collision time τ_{ei} may result from regular collisions or from interactions of the electrons with fluctuations in the electromagnetic field generated by microinstabilities in the plasma. In a collision-free plasma such as exists in the outer magnetosphere, the latter

mechanism is the only possibility of generating a finite value of σ. There is ongoing debate concerning the role of microinstabilities and the associated effective conductivity σ in unfreezing the magnetic field at the X line of a reconnection configuration in the magnetosphere. As mentioned above, such unfreezing could also be produced by the other terms on the right-hand side of Equation (22). Let us examine this possibility in detail. By use of Equation (22), the rate of change of flux, Equation (6) with $\underline{V} = \underline{v}$ may be written

$$\frac{D}{Dt}\Phi_m = -\oint_{\mathcal{L}} (\underline{E}+\underline{v}\times\underline{B})\cdot d\underline{\ell} = -E_r \ell = -\oint_{\mathcal{L}} \frac{\underline{j}}{\sigma}\cdot d\underline{\ell} - \oint_{\mathcal{L}} \frac{1}{n_e e}\,\underline{j}\times\underline{B}\cdot d\underline{\ell} + \oint_{\mathcal{L}} \frac{1}{n_e e}\,\underline{\nabla}\cdot\underline{P}_e\cdot d\underline{\ell}$$
$$- \oint_{\mathcal{L}} \frac{m_e}{n_e e^2}\left[\frac{\partial \underline{j}}{\partial t} + \underline{\nabla}\cdot(\underline{j}\underline{v} + \underline{v}\underline{j})\right]\cdot d\underline{\ell} \qquad (31)$$

where the loop $\mathcal{L}$ is shown in Figure 7. The right-hand portion of this loop is carried with the plasma towards the X line; the left-hand side is located along the X line. It is at rest because the plasma has no velocity components v_x and v_y at that location. At the right-hand part of the loop, all of the integrands on the right-hand side of (31) are negligibly small so that the field lines there are carried with the plasma in a frozen manner towards the X line.

Let us now look at the contributions to the line integrals from the portion of the $\mathcal{L}$ along the X line. A nonzero contribution from at least one of these terms is needed in order to allow reconnection and the associated transfer of the flux across the X line to occur.

(a) Unless $\sigma = \infty$ the resistive term will give a contribution.

(b) The Hall term will not contribute because $(\underline{j}\times\underline{B})\cdot d\underline{\ell} \equiv 0$ on the X line (which either has $\underline{B}=0$ or if $\underline{B}\neq 0$ is itself a field line).

(c) For a two dimensional configuration ($\frac{\partial}{\partial z} \equiv 0$) the electron pressure tensor term becomes

$$\int_A^B \frac{d\ell}{n_e e}\left[\frac{\partial P_{exz}}{\partial x} + \frac{\partial P_{eyz}}{\partial y}\right] = \frac{\ell}{n_e e}\left[\frac{\partial P_{exz}}{\partial x} + \frac{\partial P_{eyz}}{\partial y}\right]_{\substack{x=0\\y=0}} \qquad (32)$$

where ℓ is the length of the loop along the X line. Thus, only off-diagonal terms in the electron pressure tensor, caused by so-called finite Larmor radius (FLR) effects can contribute. As mentioned already, it is expected that the length scale for such effects is of the order of the electron gyroradius.

(d) The electron inertia term containing $\partial \underline{j}/\partial t$ is expected to be negligibly small unless the current is changing rapidly.

(e) For a two-dimensional symmetric configuration, the electron inertia term containing $\underline{\nabla}\cdot(\underline{j}\underline{v} + \underline{v}\underline{j})$ can be shown to yield

$$-\int_A^B \frac{m_e}{n_e e^2}\,\underline{\nabla}\cdot(\underline{j}\underline{v} + \underline{v}\underline{j})\cdot d\underline{\ell} = +\frac{m_e \ell}{n_e e^2}\, j_z\, \frac{1}{\rho}\,\frac{\partial \rho}{\partial t} \qquad (33)$$

which again vanishes for the time independent case.

We see that in the absence of a finite effective conductivity σ it is very difficult to allow flux transfer across the X line. Only FLR effects of the electrons are capable of achieving this in a steady two-dimensional geometry. In three dimensional cases the electron inertia terms may contribute also. In either case, the effects operate in a cylinder around the X line of diameter comparable to the electron inertial length or electron gyroradius. Another way to look at this is to combine $\underline{v}\times\underline{B} + \underline{j}\times\underline{B}/n_e e$

to form $\underline{v}_e \times \underline{B}$ so that

$$\frac{D\phi_m}{Dt} = -\oint (\underline{E}+\underline{v}_e\times\underline{B})\cdot d\underline{\ell} = -\oint \frac{j}{\sigma}\, d\ell + \oint \frac{1}{n_e e}\,\underline{\nabla}\cdot\underline{P}_e \cdot d\underline{\ell}$$

$$-\oint \frac{m_e}{n_e e^2}\left[\frac{\partial \underline{j}}{\partial t} + \nabla\cdot(\underline{j}\underline{v} + \underline{v}\underline{j})\right]\cdot d\underline{\ell} \qquad (34)$$

from which it is seen that for $\sigma \to \infty$ the magnetic field is frozen in the electron gas until scale lengths of the order of λ_e or R_{Le} have been produced at the X line.

The Hall current term can serve to unfreeze the magnetic field from the ion gas, i.e., from the bulk of the plasma, at distances comparable to λ_i or R_{Li} away from the X line. This is not immediately apparent since

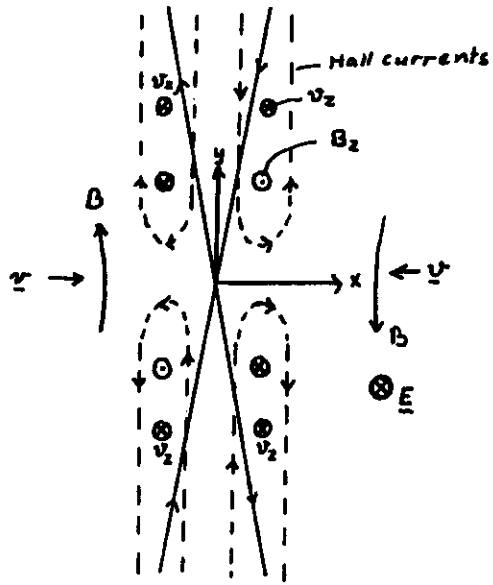

Fig. 8

in the simplest field model shown in Figure 7 the current $\underline{j}$ and the length element $d\underline{\ell}$ are parallel so that $\underline{j}\times\underline{B}\cdot d\underline{\ell} = 0$ everywhere. What is expected to happen is that the ions approaching the X line are brought nearly to a halt at a distance of order λ_i or R_{Li} from that line while the electrons continue toward that line at the field line speed E_0/B. The result of this differential motion is likely to be the formation of Hall current loops, $\underline{j}_H$, in the xy plane as illustrated in Figure 8. Denoting by $\underline{B}_\perp$ the magnetic field in the xy plane, it is seen that $\underline{j}_H\times\underline{B}\cdot d\underline{\ell}$ is now different from zero for any segment of the loop aligned with $\hat{z}$. Furthermore, the direction of $\underline{j}_H\times\underline{B}$ is the same as that of the reconnection electric field as expected.

Note that $\underline{j}_H$ has several further effects: (a) it induces a magnetic field component B_z along the z axis as shown in Figure 8; (b) the associated term $\underline{j}_H\times\hat{z}B_z$ leads to the formation of a Hall electric field $\underline{E}_H$ in the xy plane as well as to an extra force component which should produce an increased plasma pressure on the x axis near the X line; (c) the force $\underline{j}_H\times\underline{B}_\perp$ will also generate a plasma flow in the negative z direction, as shown in the figure. This flow is the macroscopic manifestation of principally the gradient drift of ions as they enter the region of nonuniform magnetic field near the X line.

SM12A-04

STRUCTURE OF RECONNECTION BOUNDARY LAYERS IN INCOMPRESSIBLE MHD

D.-J. Wang and B. U. Ö. Sonnerup (Dartmouth College, Hanover, NH 03755)

An analytical model is presented of the exit flow regions of magnetic field reconnection geometries when the reconnection rate is small. The incompressible MHD equations with nonvanishing viscosity and resistivity are simplified by use of the boundary layer approximation and the conditions are derived under which self-similar solutions of the resulting equations exist. For the case of zero viscosity and resistivity, the structure of such self-similar layers is obtained in terms of quadratures and the resulting flow and field configurations are described. Symmetric solutions relevant to reconnection in the geomagnetic tail as well as asymmetric solutions applicable to the magnetopause are found to exist. The boundary layer structure in Petschek's reconnection in the geomagnetic tail as well as asymmetric solutions applicable to the magnetopause are found to exist. The boundary layer structure in Petschek's reconnection model appears as a special case. The analysis may also apply to shear layers observed at magnetic separatrices in recent computer simulations by Biskamp and by Lee and Fu. The nature of the external flow and fields which should be matched to these boundary layer solutions is discussed briefly.

Reconnection Boundary Layers

I. Introduction

Petschek's reconnection model:

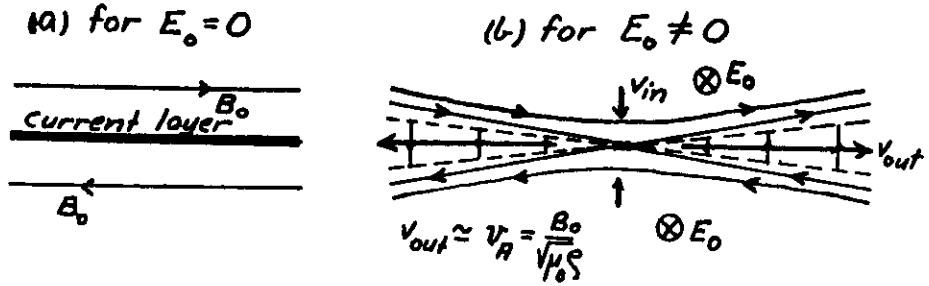

- The reconnection layer consists of two narrow wedges bounded by Alfvén waves (dashed lines) in which plasma and reconnected magnetic field flow away from the reconnection line with the Alfvén speed, $B_0/\sqrt{\mu_0 \rho}$.

- When the reconnection electric field, E_0, vanishes the wedge angle also goes to zero and the geometry reduces to that of a thin current layer with uniform but oppositely directed magnetic fields on its two sides and with no plasma flow.

- In Petschek's geometry, the outflow wedges contain a uniform flow with speed

$$v_{out} = \frac{E_0}{B_{out}} \approx \frac{B_0}{\sqrt{\mu_0 \rho}}$$

This flow is at right angles to the magnetic field, B_{out}, in the out-flow wedges. As $E_0 \to 0$, $B_{out} \to 0$ too, in such a manner that E_0/B_{out} remains constant. The wedge angle is of the order of B_{out}/B_0 and thus vanishes as $E_0 \to 0$.

- We have examined the structure of the flow and magnetic field in the outflow regions under more general assumptions than those employed by Petschek.

- We have assumed

1. Steady twodimensional reconnection

2. Incompressible MHD flow

2. The Boundary Layer Approximation

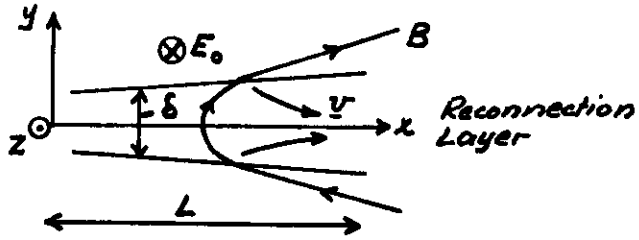

- $\frac{\partial}{\partial y} \sim \frac{1}{\delta}$ and $\frac{\partial}{\partial x} \sim \frac{1}{L}$ (Sears, 1961; Cassen and Szabo, 1970)
- $\delta \ll L$
- y component of momentum equation reduces to:

$$p + \frac{B^2}{2\mu_0} = P_\infty(x)$$

i.e., the sum of plasma pressure and magnetic pressure is constant across the layer.

- x component becomes:

$$v_x \frac{\partial v_x}{\partial x} + v_y \frac{\partial v_x}{\partial y} = -\frac{1}{\rho}\frac{\partial p}{\partial x} + \frac{1}{\mu_0 \rho} B_y \frac{\partial B_x}{\partial y} + \frac{1}{\rho}\frac{\partial}{\partial y}\mu \frac{\partial v_x}{\partial y}$$

(μ: viscosity)

- Ohm's law becomes:

$$v_x B_y - v_y B_x = E_0 - \frac{1}{\mu_0 G}\frac{\partial B_x}{\partial y}$$

(G: electrical conductivity)

- Mass and flux conservation:

$$\frac{\partial v_x}{\partial x} + \frac{\partial v_y}{\partial y} = 0 \qquad \frac{\partial B_x}{\partial x} + \frac{\partial B_y}{\partial y} = 0$$

- We introduce a streamfunction Ψ and a magnetic vector potential $(0, 0, A)$ so that

$$\underline{v} = \underline{\nabla}\Psi \times \hat{\underline{z}} \qquad \underline{B} = \underline{\nabla} A \times \hat{\underline{z}}$$

In terms of Ψ and A we then find the following two equations which describe flow and field in the layer:

$$\Psi_y \Psi_{xy} - \Psi_x \Psi_{yy} = -\frac{1}{\rho}\frac{dP_\infty(x)}{dx} + \frac{1}{\mu_0 \rho}(A_y A_{xy} - A_x A_{yy}) + (\nu \Psi_{yy})_y$$

$$-\Psi_y A_x + \Psi_x A_y = E_0 - \frac{1}{\mu_0 G} A_{yy}$$

Subscripts denote partial derivatives.

- Error is $O\left(\frac{\delta^2}{L^2}\right)$

3. Self-Similar Boundary Layer Structures

- The similarity variable is: $\eta \equiv \left(\frac{y}{x^m}\right)\left(\frac{L^m}{\delta}\right)$

- The other variables must have the form:

$$\Psi = \left(\frac{x}{L}\right)^n v_0 \delta\, f(\eta)$$

$$A = \left(\frac{x}{L}\right)^n B_0 \delta\, F(\eta)$$

$$P_\infty(x) = P_0 + K_0 \tfrac{1}{2}\rho v_0^2 \left(\frac{x}{L}\right)^q$$

$$v(x,y) = \left(\frac{x}{L}\right)^r \tilde{v}(\eta)\, v_0$$

$$G(x,y) = \left(\frac{x}{L}\right)^{-r} \tilde{G}(\eta)\, G_0$$

where $v_0 = B_0/\sqrt{\mu_0 \rho}$, $P_0 = \text{const.}$, $K_0 = \text{const.}$, $v_0 = \text{const.}$, $G_0 = \text{const.}$

- Substitution into boundary layer equations leads to consistency requirements:

$$m = 2n - 1$$
$$q = 2(1-n)$$
$$r = 3n - 2$$

n remains arbitrary!

- The two boundary-layer equations reduce to the following pair of ODEs:

$$f'^2 - \frac{n}{1-n} ff'' = F'^2 - \frac{n}{1-n} FF'' - K_0 + \frac{1}{1-n} \frac{1}{Re^*} (\tilde{\nu} f'')'$$

$$f'F - fF' = \frac{\tilde{E}_0}{n} + \frac{1}{n} \frac{1}{Rm^*} \frac{1}{G} F'' \qquad \text{(prime = derivative w.r.t. } \eta)$$

where $Re^* \equiv (\frac{\delta}{L})^2 \frac{v_0 L}{\nu_0}$ $\qquad Rm^* \equiv (\frac{\delta}{L})^2 \mu_0 G_0 v_0 L$

and $\tilde{E}_0 = \frac{E_0}{v_0 B_0} \frac{L}{\delta}$. Without loss of generality

we may choose

$$\frac{\delta}{L} = \frac{|E_0|}{v_0 B_0}$$

so that $\underline{\tilde{E}_0 = \pm 1}$. We see that the width of

the reconnection layer, δ, is proportional

to the reconnection electric field E_0.

- When the "reduced" Reynolds numbers Re^* and R_m^* are large, i.e., for large conductivity and small viscosity, the dissipative terms in the two ODEs may be dropped. The price paid for this simplification is that the structure of Alfvén waves cannot be resolved: Alfvén waves will then appear as discontinuities.

4. Structure of Nondissipative Layers

- The equations reduce to the form

$$f'^2 - F'^2 = \frac{n}{1-n}(ff'' - FF'') - K_0$$
$$f'F - fF' = \tilde{E}_0/n \qquad (\tilde{E}_0 = \pm 1)$$

- To solve these equations, let

$$\left.\begin{aligned} U &\equiv F + f \\ V &\equiv F - f \end{aligned}\right\} \text{ and } \quad Y \equiv UV = F^2 - f^2$$

- In terms of these new variables the two equations become (after simple rearrangements):

$$\begin{cases} U'V' = \frac{n}{2} Y'' + (1-n)K_0 \\ Y' - 2UV' = 2VU' - Y' = \frac{2}{n}\tilde{E}_0 \end{cases}$$

The second equation gives (*) $\begin{cases} UV' = \frac{1}{2}Y' - \frac{\tilde{E}_0}{n} \\ U'V = \frac{1}{2}Y' - \frac{\tilde{E}_0}{n} \end{cases}$

If we multiply the first equation by $UV = Y$ and make use of these expressions for UV' and $U'V$, we find (using also $Y'' \equiv \frac{d}{dY}(\frac{1}{2}Y'^2)$)

$$\frac{1}{4}Y'^2 - \frac{1}{n^2} = \frac{n}{2} Y \frac{d}{dY} \frac{1}{2} Y'^2 + (1-n)K_0 Y$$

- This is a linear nonhomogeneous first-order differential equation for Y'^2 with Y as the independent variable. Its solution is

$$Y' = \pm 2\sqrt{C|Y|^{1/n} + K_0 Y + 1/n^2} \qquad (1)$$

where C = const. of integration. One further integration gives

$$\pm \frac{1}{2}\int_{Y_0}^{UV} \frac{dY}{\sqrt{C|Y|^{1/n} + K_0 Y + 1/n^2}} = \eta - \eta_0 \qquad (2)$$

- Finally, we form the ratio of the two eq's (*):

$$\frac{UV'}{U'V} = \frac{U\,dV}{V\,dU} = \frac{Y'/2 - \tilde{E}_0/n}{Y'/2 + \tilde{E}_0/n} \equiv G(Y) \qquad (3)$$

(using (1))

This may be rearranged to

$$\frac{dY}{dU} = \frac{Y}{U}(G+1) \quad \text{or} \quad \frac{dY}{dV} = \frac{Y}{V}(1+G^{-1})$$

Thus $\frac{dU}{U} - \frac{dV}{V} = \frac{dY}{Y}\left[\frac{1}{G+1} - \frac{1}{1+G^{-1}}\right] = \frac{dY}{Y}\frac{1-G}{1+G}$

Substitute the expression (3) for G and integrate:

$$\ln\left|\frac{U}{V}\right| = \pm\frac{\tilde{E}_0}{n}\int_{Y_0}^{UV} \frac{dY}{Y\sqrt{C|Y|^{1/n} + K_0 Y + 1/n^2}} + \ln\left|\frac{U_0}{V_0}\right| \qquad (4)$$

- Equations (2) and (4) are the general solution of the nondissipative case in parametric form: Choose a value of UV; find η from (2) and U/V from (4); find U and V separately and use $U = F+f$, $V = F-f$.

- We may remove the constant C from (2) and (4) by the transformation

$$\tilde{Y} \equiv |C|^n Y \qquad \tilde{\eta} \equiv |C|^n \eta \qquad \tilde{K}_0 \equiv K_0/|C|^n$$

to get a discriminant of the form

$$H(\tilde{Y}) = \pm|\tilde{Y}|^{1/n} + \tilde{K}_0\tilde{Y} + \frac{1}{n^2}$$

The properties of the solution are determined principally by the properties of $H(\tilde{Y})$.

- 4 different regions in the $\tilde{K}_0 n$ plane as shown in Fig. 1.

- $H = 0$ at center of symmetric layer

- $Y = F^2 - f^2 = 0$ at Alfvén waves

$\therefore 0 < n < 2$

$0 < n \le 1$	v_x, B_x finite at Alfvén wave
$1 < n < 2$	v_x, B_x infinite — energy finite
$0 > n > 2$	energy infinite

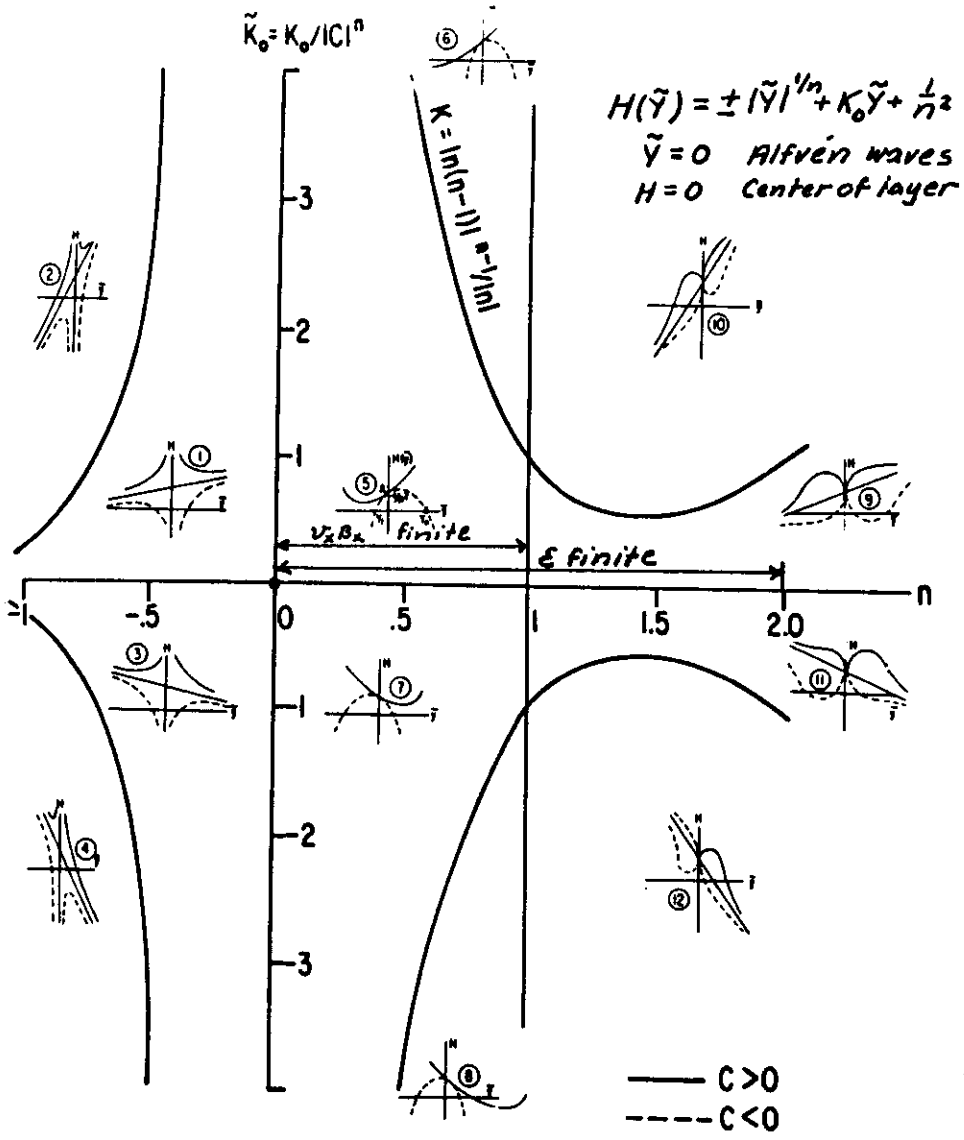
$\tilde{K}_0 = K_0/|C|^n$
$H(\tilde{Y}) = \pm|\tilde{Y}|^{1/n} + K_0\tilde{Y} + \frac{1}{n^2}$
$\tilde{Y} = 0$ Alfvén waves
$H = 0$ Center of layer
$K = \ln|n-1|\, n^{-1/\ln|}$
$v_z B_z$ finite
$\mathcal{E}$ finite
n
-.5
0
.5
1
1.5
2.0
3
2
1
-1
-2
-3
C>0
C<0

Fig. 1

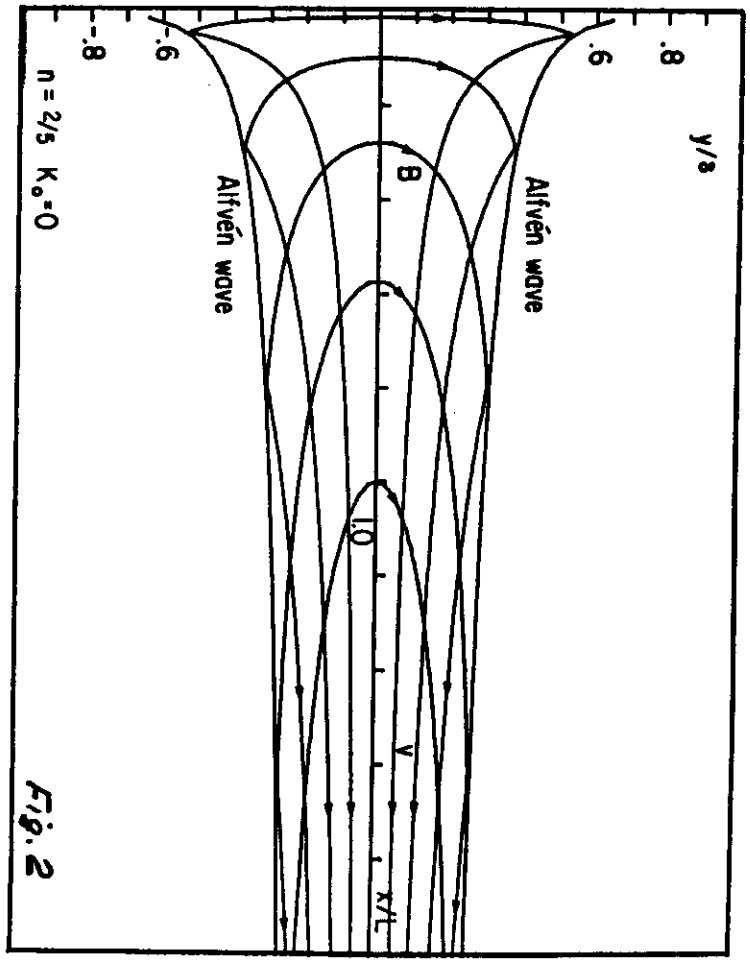
n = 2/5 K_0=0
-.8
-.6
.6
.8
y/a
Alfvén wave
Alfvén wave
B
1.0
V
x/L

Fig. 2

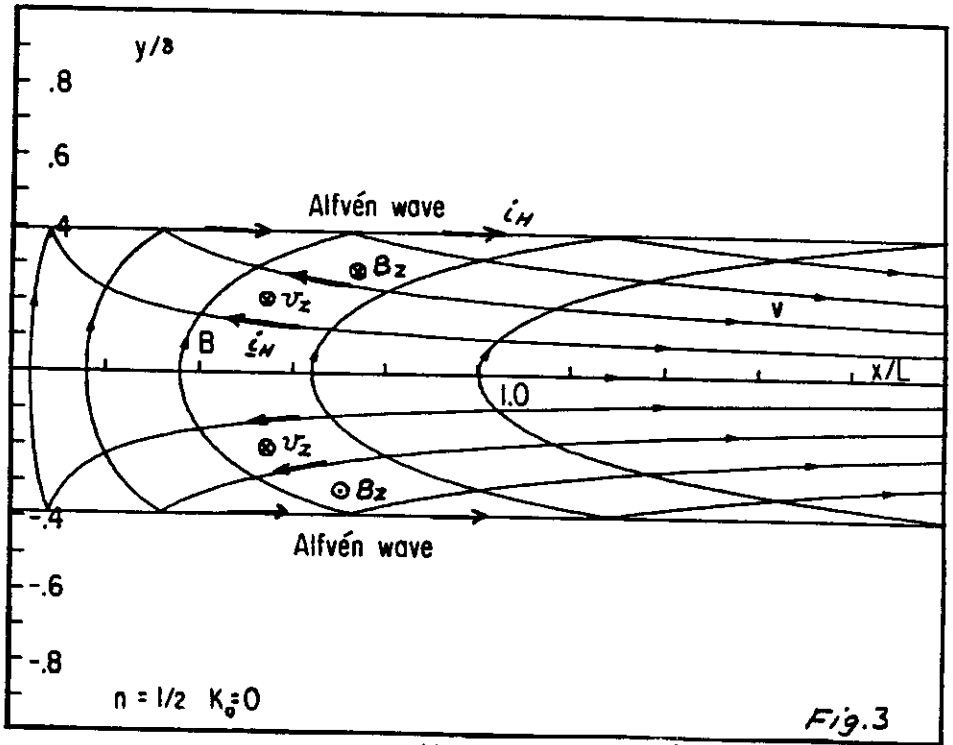

Fig.3

Hall currents i_H : see page 19.

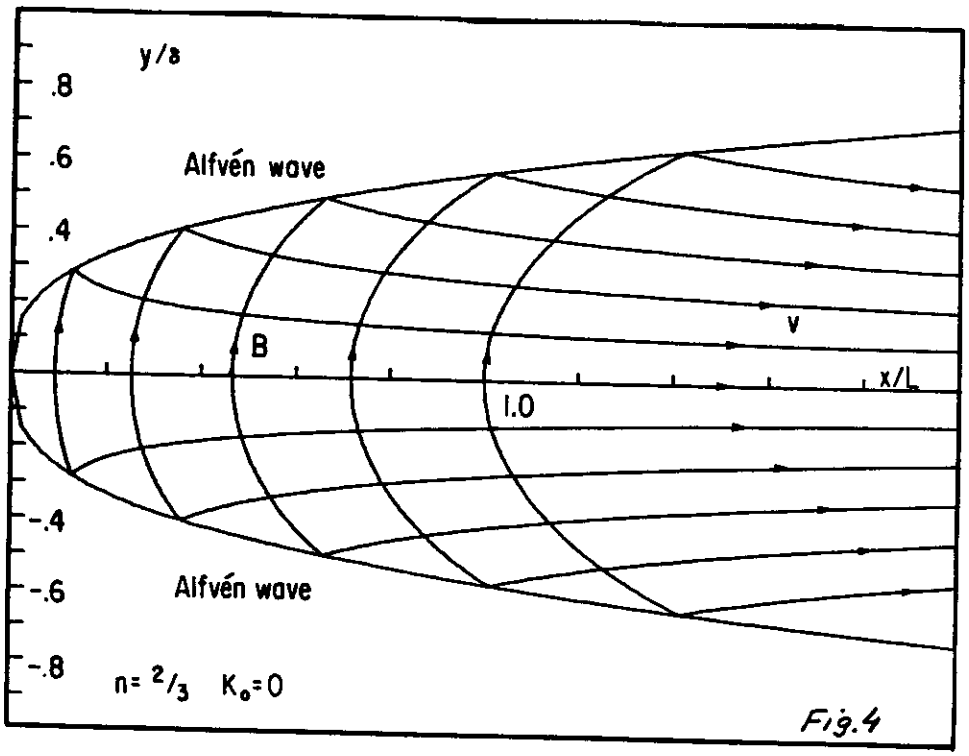

Fig.4

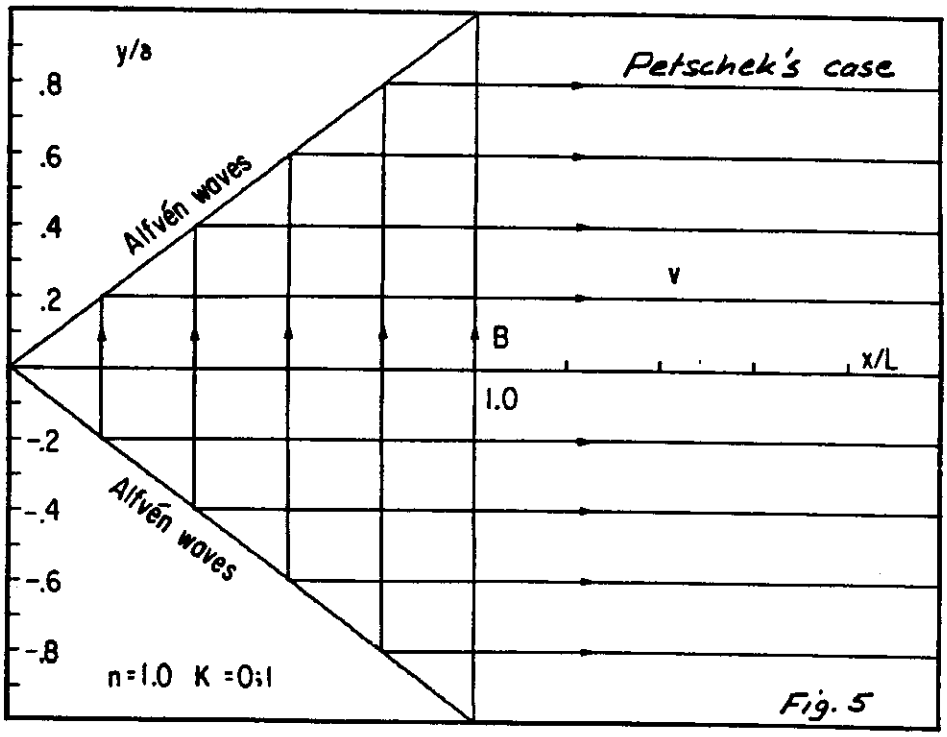
y/a
.8
.6
.4
.2
-.2
-.4
-.6
-.8
Alfvén waves
Alfvén waves
Petschek's case
v
B
x/L
1.0
n=1.0 K =0;1

Fig. 5

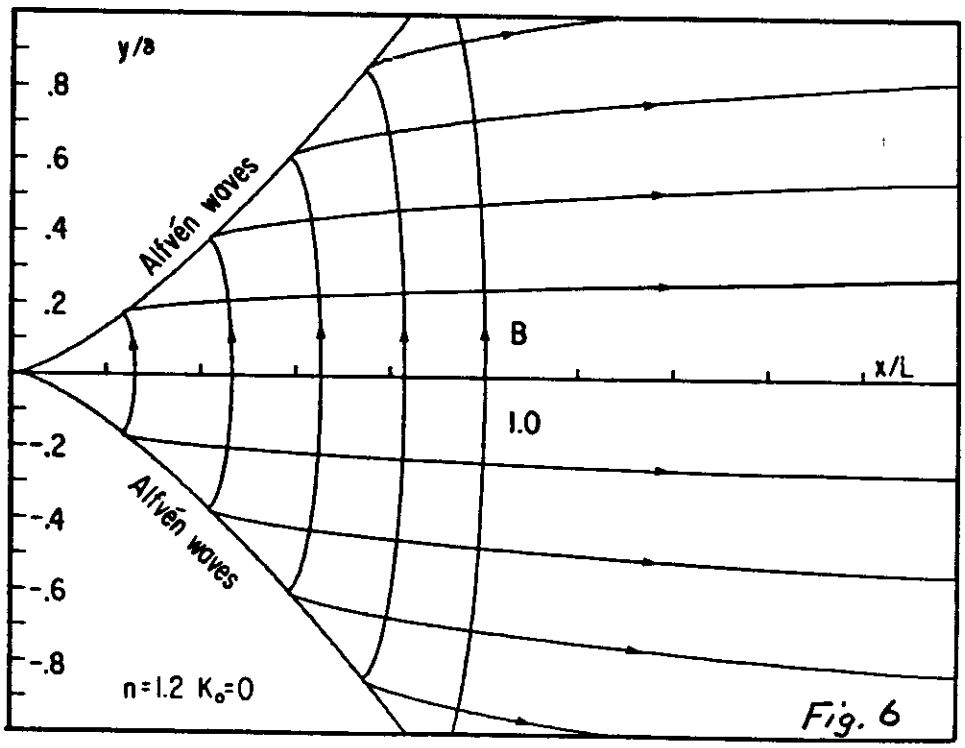
y/a
.8
.6
.4
.2
-.2
-.4
-.6
-.8
Alfvén waves
Alfvén waves
B
x/L
1.0
n=1.2 K₀=0

Fig. 6

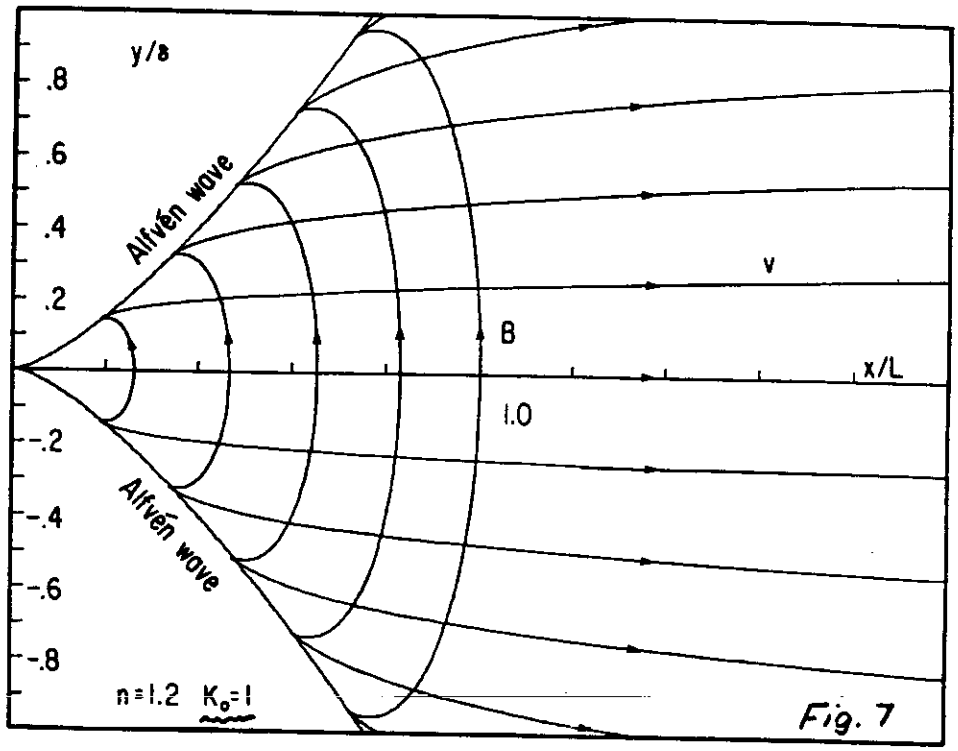

Fig. 7

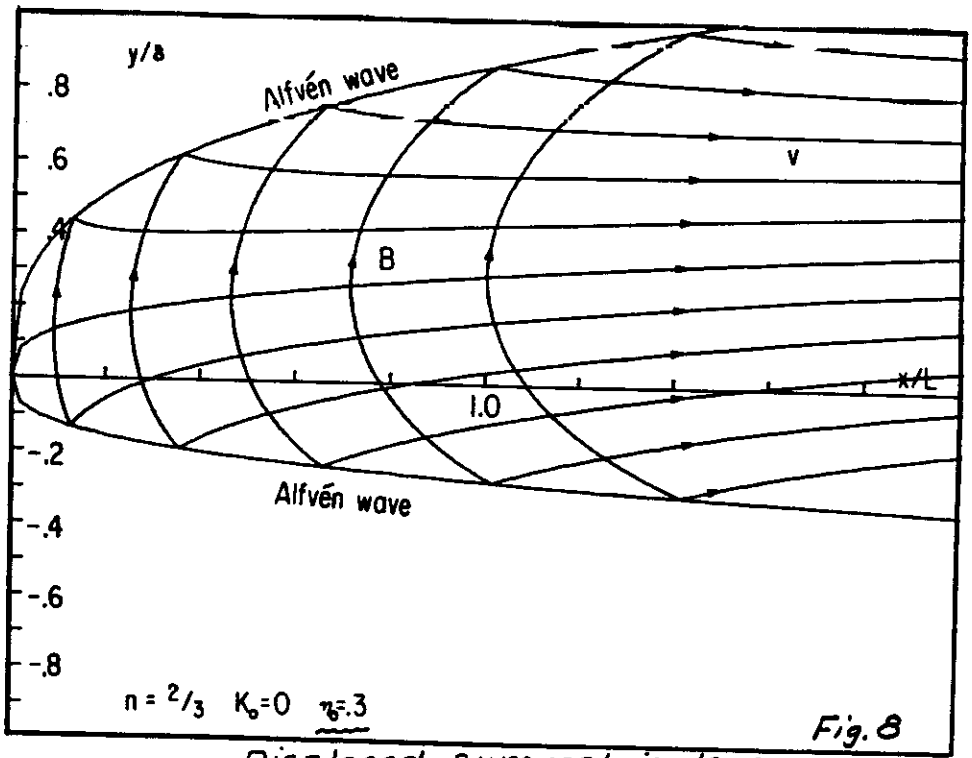

Fig. 8

Displaced symmetric layer

5. The Case $n = 1/2$

- The boundary layer thickness is independent of x!

- Analytical solutions ($\tilde{E}_0 = -1$ say):

$$\left.\begin{aligned} F &= A_1 \cos\alpha\eta + A_2 \sin\alpha\eta \\ f &= a_1 \cos\alpha\eta + a_2 \sin\alpha\eta \end{aligned}\right\} \rightarrow \begin{cases} a_1 A_2 - a_2 A_1 = \frac{2}{\alpha} \\ a_1^2 + a_2^2 = A_1^2 + A_2^2 - \frac{K_0}{\alpha^2} \end{cases}$$

or

$$\left.\begin{aligned} F &= A_3 e^{\alpha\eta} + A_4 e^{-\alpha\eta} \\ f &= a_3 e^{\alpha\eta} + a_4 e^{-\alpha\eta} \end{aligned}\right\} \rightarrow \begin{cases} a_3 A_4 - a_4 A_3 = -\frac{1}{\alpha} \\ a_3 a_4 = A_3 A_4 + \frac{K_0}{4\alpha^2} \end{cases}$$

For example, for a symmetric layer with $K_0 = 0$:

$$\left.\begin{aligned} F &= -\cos 2\eta \\ f &= +\sin 2\eta \end{aligned}\right\} \text{ Alfvén waves at } \eta = \pm\frac{\pi}{8}$$

- Hall effect for this example:

$$\left.\begin{aligned} B_z &= -2B_0 \frac{\lambda_i}{\delta} \sqrt{\frac{x}{L}} \sin 2\eta \\ v_z &= -2 v_0 \frac{\lambda_i}{\delta} \sqrt{\frac{x}{L}} \cos 2\eta \\ \phi_H &= -v_0 B_0 \lambda_i \frac{x}{L} \cos 4\eta \end{aligned}\right\}$$

Hall currents along streamlines: Fig. 3
Closure on Alfvén wave.

$$\lambda_i \equiv \sqrt{m_i/\mu_0 n e^2}$$ (1)

5. External Field and Flow

- Unperturbed case, i.e., $E_0 = 0$:

$\underline{v}_\infty$ and $\underline{B}_\infty$ are parallel and, in the simplest case, may be chosen as potential fields in a wedge region of angle θ. At $y = 0$ we then have

$$B_{\infty x} \sim v_{\infty x} \sim x^{1-n} \quad \text{for } \theta = \frac{\pi}{2-n}$$

and $$P_\infty(x) = p_{stagn} + \frac{\rho}{2}\left[\frac{B_{\infty x}^2(x)}{\mu_0} - v_{\infty x}^2(x)\right]$$

$\because$ { Subalfvénic unperturbed flow $\supset K_0 > 0$
Superalfvénic -"- -"- $\supset K_0 < 0$

Ex 1 $n = 1$ gives $\theta = \pi$ Petschek's case
Ex 2 $n = \frac{1}{2}$ gives $\theta = \frac{2}{3}\pi$ Case discussed in section 5 and Fig. 3

The unperturbed geometry is shown in Fig. 9a.

- Perturbed case, i.e., E_0 nonzero but small:

✓ Qualitative behavior is shown in Fig. 9b.
✓ Quantitative analysis is not yet complete.

✓ This is a singular perturbation problem: large perturbations in $\underline{v} \cdot \hat{\underline{B}}$ occur even when E_0 is small.

✓ This effect leads to the formation of "separatrix layers", an effect that has been observed in simulations (e.g., Lee-Fu, 1986; Biskamp, 1986) and has been explained by Soward-Priest (1986) and Schindler-Birn (1987).

✓ The present analysis can describe not only the reconnection layer in Fig. 9b but the separatrix layers as well. (As a simple illustration, note that for $K_0 = 0$ fieldlines and streamlines can be interchanged, e.g. in Fig. 3)

7. Conclusion

- Generalization to Petschek's reconnection boundary layer has been found.
- New solutions correspond to external "wedge" field and flow.
- Generally they show strong field-aligned flows in the boundary layer
- Separatrix-layer solutions can also be produced.

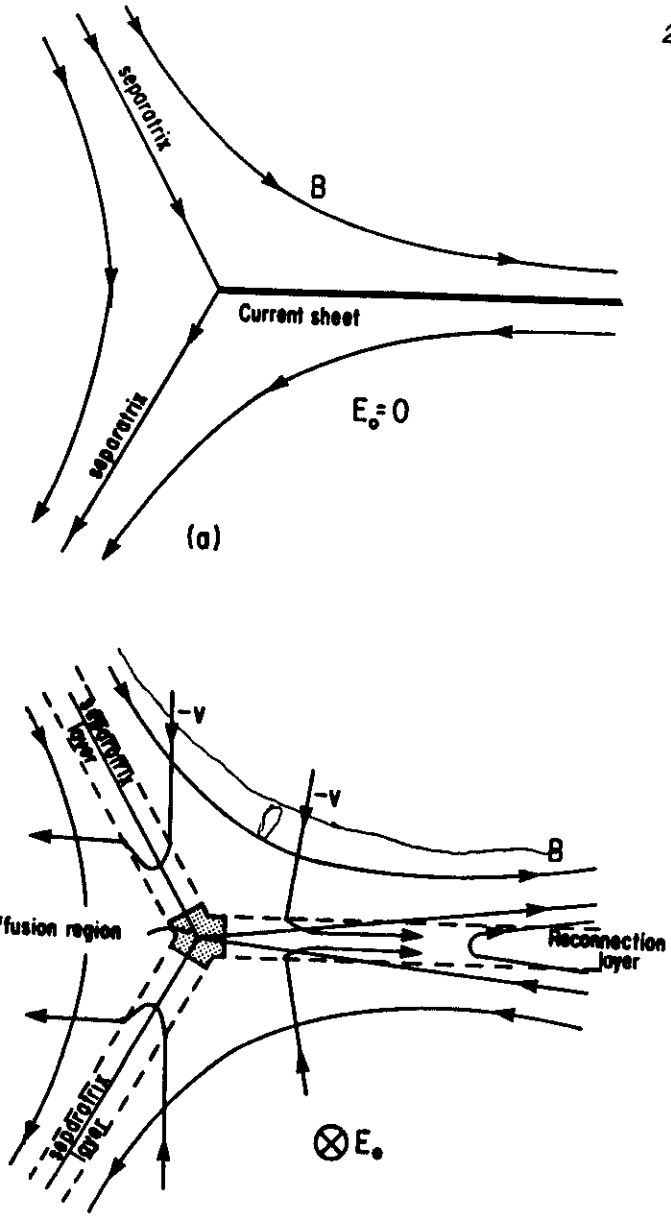

Fig. 9

References

Biskamp, D., Phys. Fluids, 29, 1520, 1986.

Cassen, P., and J. Szabo, Planet. Space Sci., 18, 349, 1970.

Lee, L.C., and Z.F. Fu, J.G.R., 91, 6807, 1986.

Petschek, H.E., NASA-SP 50, 425, 1964.

Schindler, K., and J. Birn, J.G.R., 92, 95, 1987.

Sears, W.R., Astronaut. Acta, 7, 223, 1961.

Soward, A.M., and E.R. Priest, J. Plasma Phys., 35, 333, 1986.

Acknowledgment

Research supported by NSF under grant ATM-8507192 to Dartmouth College.